

Journal Pre-proof

Discovery of sulfonyl hydrazone derivative as a new selective PDE4A and PDE4D inhibitor by lead-optimization approach on the prototype LASSBio-448: *In vitro* and *in vivo* preclinical studies

Isabelle Karine da Costa Nunes, Everton Tenório de Souza, Italo Rossi Roseno Martins, Gisele Barbosa, Manoel Oliveira de Moraes Junior, Millena de Melo Medeiros, Sheyla Welma Duarte Silva, Tatiane Luciano Balliano, Bagnólia Araújo da Silva, Patrícia Machado Rodrigues Silva, Vinicius de Frias Carvalho, Marco Aurélio Martins, Lidia Moreira Lima

PII: S0223-5234(20)30464-5

DOI: <https://doi.org/10.1016/j.ejmech.2020.112492>

Reference: EJMECH 112492

To appear in: *European Journal of Medicinal Chemistry*

Received Date: 18 March 2020

Revised Date: 9 May 2020

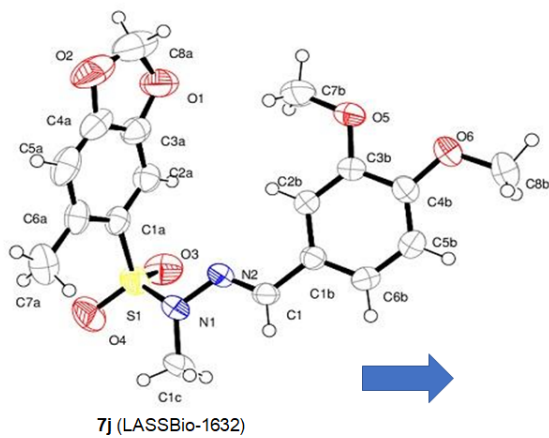
Accepted Date: 19 May 2020

Please cite this article as: I. Karine da Costa Nunes, E. Tenório de Souza, I.R. Roseno Martins, G. Barbosa, M. Oliveira de Moraes Junior, M. de Melo Medeiros, S.W. Duarte Silva, T.L. Balliano, B. Araújo da Silva, P.M. Rodrigues, Silva, V. de Frias Carvalho, M.A. Martins, L.M. Lima, Discovery of sulfonyl hydrazone derivative as a new selective PDE4A and PDE4D inhibitor by lead-optimization approach on the prototype LASSBio-448: *in vitro* and *in vivo* preclinical studies, *European Journal of Medicinal Chemistry*, <https://doi.org/10.1016/j.ejmech.2020.112492>.

This is a PDF file of an article that has undergone enhancements after acceptance, such as the addition of a cover page and metadata, and formatting for readability, but it is not yet the definitive version of record. This version will undergo additional copyediting, typesetting and review before it is published in its final form, but we are providing this version to give early visibility of the article. Please note that, during the production process, errors may be discovered which could affect the content, and all legal disclaimers that apply to the journal pertain.

© 2020 Elsevier Masson SAS. All rights reserved.



**Drug-like properties:**

M.W. = 392.43
 LogP = 3.0
 tPSA = 95.04
 Aq. solubility = 0.5 μM
 Stable at pH = 7.4 and pH = 2.0
 Pe (PAMPA-BBB) = 6.52×10^{-6} cm/s
 Pe (PAMPA-TGI) = 13.08×10^{-6} cm/s

Enzymatic Assay:

IC_{50} (PDE4A) = 0.5 ± 0.01 μM
 IC_{50} (PDE4D) = 0.7 ± 0.02 μM

Phenotypic Assays: it reduced LPS-induced airway hyper-reactivity (AHR) and TNF- α production in the lung tissue and relaxed the guinea pig trachea pre-contracted with CCh in both the presence and absence of epithelium.

Discovery of sulfonyl hydrazone derivative as a new selective PDE4A and PDE4D inhibitor by lead-optimization approach on the prototype LASSBio-448: *in vitro* and *in vivo* preclinical studies

Isabelle Karine da Costa Nunes^{1,2,3}, Everton Tenório de Souza^{2,4}, Italo Rossi Roseno Martins^{5,6}, Gisele Barbosa^{1,2}, Manoel Oliveira de Moraes Junior^{1,2}, Millena de Melo Medeiros⁵, Sheyla Welma Duarte Silva⁸, Tatiane Luciano Balliano⁸, Bagnólia Araújo da Silva^{5,7}, Patrícia Machado Rodrigues and Silva^{1,2,4}, Vinicius de Frias Carvalho⁴, Marco Aurélio Martins^{1,2,4*}, Lídia Moreira Lima^{1,2*}

¹Instituto Nacional de Ciência e Tecnologia de Fármacos e Medicamentos (INCT-INOVAR; <http://www.inct-inofar.ccs.ufrj.br/>). Universidade Federal do Rio de Janeiro, Laboratório de Avaliação e Síntese de Substâncias Bioativas (LASSBio®, <http://www.farmacia.ufrj.br/lassbio/>), CCS, Cidade Universitária, P.O. Box 68024, ZIP: 21941-971, Rio de Janeiro-RJ, Brasil

²Programa de Pós-graduação em Farmacologia e Química Medicinal, Instituto de Ciências Biomédicas, Universidade Federal do Rio de Janeiro, Rio de Janeiro, RJ, Brasil

³Laboratório de Apoio ao Desenvolvimento Tecnológico-LADETEC. Instituto de Química, Universidade Federal do Rio de Janeiro, RJ, Brasil

⁴Laboratório de Inflamação, Instituto Oswaldo Cruz-Fiocruz, Fundação Oswaldo Cruz, Rio de Janeiro, RJ, 21045-900, Brasil

⁵Programa de Pós-graduação em Produtos Naturais e Sintéticos Bioativos, Centro de Ciências da Saúde, Universidade Federal da Paraíba, João Pessoa, Brasil.

⁶Departamento de Medicina, Campus Senador Helvécio Nunes de Barros, Universidade Federal do Piauí, Picos, Brasil.

⁷Departamento de Ciências Farmacêuticas, Centro de Ciências da Saúde, Universidade Federal da Paraíba, João Pessoa, Brasil.

⁸Laboratório de Cristalografia Bioprocessos e Modelagem Molecular – LaBioCriMM. Instituto de Química e Biotecnologia, Universidade Federal de Alagoas, AL, Brasil.

*Address for correspondence: Dr. Lídia Moreira Lima, Universidade Federal do Rio de Janeiro, Centro de Ciências da Saúde, Bloco B, sala 14, P.O. Box 68024, Rio de Janeiro, RJ, Brasil, ZIP Code: 21941-902

PH/FAX 55-21-39386503. Email: lidialima@ufrj.br or lmlima23@gmail.com; and Dr. Marco Aurélio Martins, Laboratório de Inflamação, Instituto Oswaldo Cruz-Fiocruz, Rio de Janeiro, RJ, Brasil, ZIP Code: 21040-360
PH/FAX 55-21-25621358. Email: mam2856@gmail.com

Abstract

Phosphodiesterase 4 (PDE4) inhibitors have emerged as a new strategy to treat asthma and other lung inflammatory diseases. Searching for new PDE4 inhibitors, we previously reported the discover of LASSBio-448, a sulfonamide with potential to prevent and reverse pivotal pathological features of asthma. In this paper, two novel series of sulfonamide (**6a-6m**) and sulfonyl hydrazone (**7a-7j**) analogues of LASSBio-448 have been synthesized and evaluated for selective inhibitory activity toward cAMP-specific PDE4 isoforms. From these studies, we have identified **7j** (LASSBio-1632) as a new anti-asthmatic lead-candidate associated with selective inhibition of PDE4A and PDE4D isoenzymes and blockade of airway hyper-reactivity (AHR) and TNF- α production in the lung tissue. In addition, it was able to relax guinea pig trachea on non-sensitized and sensitized animals and showed great TGI permeability.

Keywords: asthma; PDE4; LASSBio-448; sulfonyl hydrazone; sulfonamide;

lead-optimization

1. Introduction

Phosphodiesterase (PDE) isoenzymes act by promoting the hydrolysis and subsequent inactivation of the second-messenger molecules cyclic 3',5'-adenosine monophosphate (cAMP) and cyclic 3',5'-guanosine monophosphate (cGMP). They have been organized into at least 11 families (PDE1 to PDE11) based on a variety of criteria including substrate specificity, inhibitor sensitivity and sequence homogeneity [1]. Each member within the PDE4 subfamily (PDE4A to PDE4D) specifically targets cAMP and are mainly expressed in immunocompetent cells (e.g. T cells, monocytes, macrophages, neutrophils, dendritic cells and eosinophils), brain, cardiovascular tissues, smooth muscles and keratinocytes [2].

Targeting PDE4 has therapeutic potential as treatment for several inflammatory conditions, including acute lung injury, chronic obstructive pulmonary disease (COPD) and asthma, because cAMP intracellular elevation following PDE4 blockade strongly correlates with the inhibition of innate and adaptive immune responses which are over activated in these diseases. Existing evidence indicates that PDE4 inhibition led to accumulation of cAMP and anti-inflammatory activity in many cell types, i.e., macrophages, T cells, neutrophils, monocytes, eosinophils and dendritic cells, mediated by several downstream key elements, such as PKA, cyclic nucleotide-gated ion channels, and/or Epac 1/2 [3-6].

Several PDE4 inhibitors have been described in literature [7-10] (Chart 1). Among them roflumilast is approved to treat severe COPD in patients with chronic bronchitis and frequent exacerbations. Nevertheless, the clinical dosage and efficacy of roflumilast is limited by target-related side effects, including nausea, diarrhea, and headaches (Garnock-Jones, 2015) (doi: 10.1007/s40265-015-0463-1). As the most inflammatory cells abundantly express only PDE4A, PDE4B, and PDE4D isoforms, it is very important to develop new therapeutic strategies based on the selective inhibition of PDE4 isoforms to reduce or prevent the adverse effects caused by non-specific PDE4 inhibition. At the time, several PDE4B and PDE4D inhibitors with potential clinical efficacy and minimal systemic adverse effects are under development for the treatment of clinical inflammatory diseases.

As part of a research program aimed at the discovery of new anti-inflammatory drug candidates, we describe here the attempt to optimize the prototype LASSBio-448 (**5**, Chart 1), previously reported to inhibit all PDE4 isoforms, though being about 4-fold less potent concerning blockade of PDE4D as compared to the other three PDE4 subtypes. Furthermore, given orally, LASSBio-448 prevented airway hyper-reactivity and lung inflammation triggered by allergen and LPS [10]. In this context, our goals were to synthesize two series of sulfonamides (**6a-6l**) and sulfonyl hydrazones (**7a-7j**), designed as LASSBio-448 structural analogues, and to assess their PDE4 inhibitory effect, drug likeness profile and anti-inflammatory activity in a murine model of pulmonary inflammation [10].

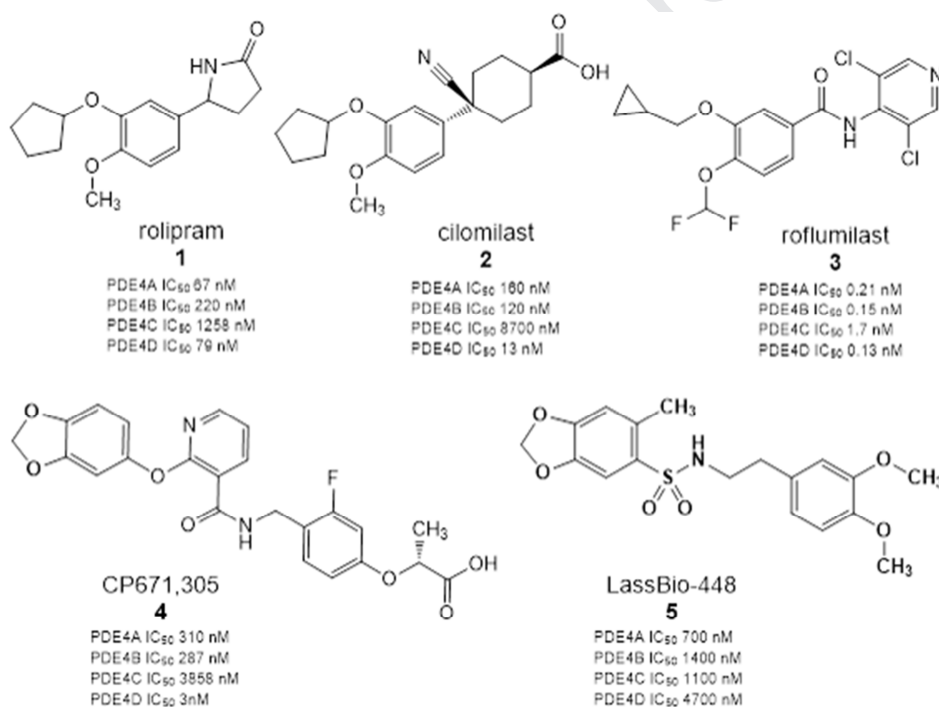


Chart 1. Examples of PDE4 inhibitors bearing different structural patterns. Data taken from references: [7-10]

The design conception of the sulfonamides (**6a-6l**) considered molecular modifications at the structure of the prototype LASSBio-448 (**5**). The modifications were based on bioisosteric replacement of benzodioxole ring (**a**, Fig. 1) by ring opening and monovalent group exchange strategies [11]. The replacement of the ethylene (CH₂CH₂) linker by imine (N=CH) unit allowed the design conception of sulfonyl hydrazone series (**7a-7j**). Further, to investigate

methyl effect [12], on PDE4 inhibitory activity, the homologation of the N sp³ (by the introduction of a methyl group) was proposed (Fig. 1).

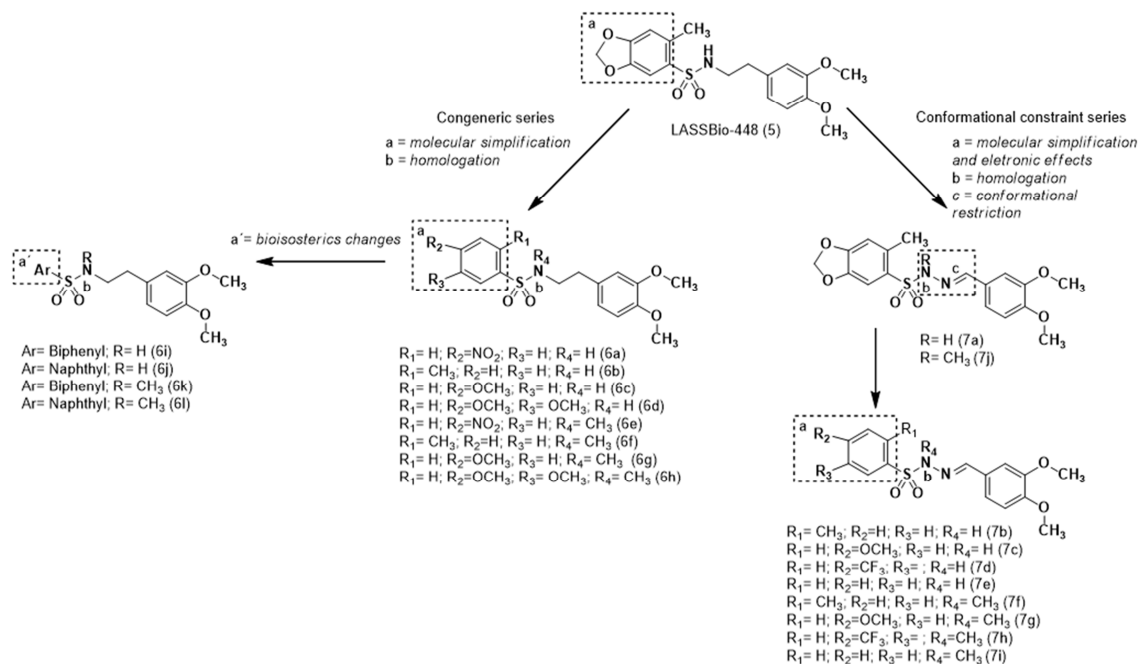


Fig. 1. Genesis concept of sulfonamides (**6a-6l**) and sulfonyl hydrazones (**7a-7j**) designed by molecular modification on PDE4 inhibitor LASSBio-448 (**5**).

2. Materials and Methods

2.1 Synthesis and Characterization

2.1.1 Chemical

Reagents and solvents were purchased from commercial suppliers and used as received. The progress of all reactions was monitored by thin layer chromatography (TLC), which was performed on 2.5 × 7.5 cm² aluminum sheets precoated with silica gel 60 (HF-254, E. Merck) to a thickness of 0.25 mm. The developed chromatograms were viewed under ultraviolet light (254 nm). IR spectra (cm⁻¹) were taken on FTLA spectrometer in KBr discs. Elemental analyses were carried out on a Thermo Scientific Flash EA 1112 Series CHN-Analyzer. HRMS analyses were carried out on a Q-Exactive Orbitrap mass spectrometer (MS) (Thermo Fisher Scientific, Bremen, Germany)

operating by switching between positive and negative ionization modes and equipped with an Electrospray Ionization (ESI) source.

Analytical HPLC was used for compound purity and stability determinations using Shimadzu LC-20AD with or Kromasil 100-5C18 (4.6 mm × 250 mm) and a Shimadzu SPD-M20A detector at 254 nm wavelength. The solvent system used for HPLC analyses was acetonitrile: water (70:30 and 60:40), with or without of 0.1% trifluoroacetic acid. The isocratic HPLC mode was used, and the flow rate was 1.0 mL/min. The purity of compounds was found to be greater than 95%. ^1H e ^{13}C NMR were determined using a 200/50 MHz Bruker DPX-200/DPX-300 or 500/125 MHz Varian 400-Mr spectrometer, respectively, in DMSO or CDCl_3 deuterated containing ca. 1% tetramethylsilane as an internal standard. The peak positions are given in parts per million (δ ppm), and J values are given in hertz. Signal multiplicities are represented by: s (singlet), d (doublet), t (triplet), q (quartet), m (multiplet) and br (broad signal). Melting points were determined with a Quimis 340 apparatus and are uncorrected. The HPLC solvents (methanol, acetonitrile and dimethylsulfoxide) were purchased from Sigma-Aldrich (St. Louis, MO, USA). Water used in the preparations has been previously purified and filtered using a Milli-Q system (Millipore, St Quentin-en-Yvelines, France).

X-ray diffraction was performed from the diffracted intensity measurements of the samples obtained using the KappaCCD diffractometer [KappaCCD Enraf-Nonius] (IQ-UFAL). Data analysis was performed using the WINGX program.

Magnesium sulfate (MgSO_4), calcium chloride (CaCl_2), potassium chloride (KCl), sodium chloride (NaCl), glucose, sodium bicarbonate (NaHCO_3),

hydrochloric acid (HCl), potassium monobasic phosphate (KH₂PO₄) and sodium hydroxide (NaOH) were purchased from Vetec Química Fina Ltda. Solutions of these substances, except for glucose, NaCl and NaHCO₃, were prepared in distilled water and kept under refrigeration.

2.2. General procedure for the preparation of sulfonamides

Sulfonamides **6a-l** were prepared by a condensation reaction between the corresponding sulfonyl chloride derivative (1mmol), which was solubilized in dichloromethane (15 mL), containing 50 μ L of triethylamine, with the respective functionalized amines: 3,4-dimethoxyphenethylamine and *N*-methyl-3,4-dimethoxyphenethylamine (1 mmol) to obtain **6a-d**, **6i-j** and **6e-h**, **6k-l**, respectively. The mixture was stirred at room temperature for 2-3h. Afterward, the isolation was carried out with dilution using 10mL of dichloromethane and extracted with aqueous HCl 10% (four times with 10 ml each time). The organic phase was dried with addition of anhydrous sodium sulfate, filtered and concentrated under reduced pressure to obtain the compounds. Yields and characterization pattern are described below:

2.2.1. *N*-(3,4-dimethoxyphenethyl)-4-nitrobenzenesulfonamide (LASSBio-1629, 6a)

The title compound was obtained in 59% yield, by condensing 4-nitrobenzenesulfonyl chloride with 3,4-dimethoxyphenylethylamine, as a yellow powder with mp 107-109 °C.

IR (KBr) cm⁻¹: 3261; 3102; 3037; 3000; 2962; 2933; 2869; 2839; 1606; 1595; 1532; 1515; 1448; 1422; 1353; 1342; 1256; 1233; 1167; 1139; 1092; 1024; 974; 945; 902; 854; 817; 765; 741; 682; 614.

¹H NMR (400 MHz, DMSO-*d*₆) δ (ppm): 2.59 (t, 2H, ³*J* 7.1 Hz; 3.05 (q, 2H, ³*J* 7.1 Hz; 3.66 (s, 6H); 6.61 (dd, 1H, ³*J* 8.1 Hz, ⁴*J* 1.9 Hz); 6.66 (d, 1H, ⁴*J* 1.9 Hz); 6.74 (d, 1H, ³*J* 8.1 Hz); 7.92 (d, 2H, ³*J* 8.9 Hz); 8.03 (t, 1H, ³*J* 5.6 Hz); 8.31 (d, 2H, ³*J* 8.9 Hz);

¹³C NMR (125 MHz, DMSO-*d*₆) δ (ppm): 35.2; 44.7; 55.7; 55.8; 112.1; 112.9; 121; 124.8; 128.3; 131.2; 146.7; 147.7; 148.8, 149.7;

CHN: C₁₆H₁₈N₂O₆S; calculated C 52.45%; H 4.95%; N 7.65% and determined C 52.77%; H 4.97%; N 7.47%.

HPLC: 60/40 acetonitrile/water; λ 254 nm: 98.8% purity.

2.2.2. *N*-(3,4-dimethoxyphenethyl)-2-methylbenzenesulfonamide (LASSBio-1613, 6b)

The title compound was obtained in 70% yield, by condensing *o*-toluenesulfonyl chloride with 3,4-dimethoxyphenethylamine, as a yellow powder with mp 78-80 °C.

IR (KBr) (cm⁻¹): 3277; 2983; 2966; 2928; 2837; 1594; 1517; 1466; 1443; 1428; 1360; 1347; 1316; 1262; 1235; 1154; 1102; 1029; 940; 894; 851; 816; 164; 779; 713; 686; 632.

¹H NMR (200 MHz, DMSO-*d*₆) δ (ppm): 2.49 (s, 3H); 2.56 (t, 2H, *J* 7.6 Hz); 2.96 (q, 2H, *J* 7.6 Hz); 3.67 (s, 3H); 3.68 (s, 3H); 6.57 (dd, 1H, ³*J* 8.1 Hz, ⁴*J* 1.9 Hz); 6.65 (d, 1H, ⁴*J* 1.8 Hz); 6.77 (d, 1H, ³*J* 8.1 Hz); 7.33 (m, 2H); 7.48 (td, 1H, ³*J* 7.4 Hz, ⁴*J* 1.2 Hz); 7.68 (t, 1H, ³*J* 5.7 Hz, NH); 7.35 (dd, 1H, ³*J* 8.4 Hz, ⁴*J* 1.4 Hz);

¹³C NMR (50 MHz, DMSO-*d*₆) δ (ppm): 20.2; 35.3; 44.4; 55.8; 56; 112.3; 112.8; 120.9; 126.5; 128.8; 131.5; 132.7; 132.9; 137; 139.1; 147.7; 149.

CHN: C₁₇H₂₁NO₄S; calculated C 60.87%; H 6.31%; N 4.18% and determined C 60.68%; H 6.35%; N 4.26%.

HPLC: 60/40 acetonitrile/water; λ 254 nm: 97.3% purity

2.2.3. N-(3,4-dimethoxyphenethyl)-4-methoxybenzenesulfonamide (LASSBio-1625, 6c)

The title compound was obtained in 73% yield, by condensing 4-methoxybenzenesulfonyl chloride with 3,4-dimethoxyphenylethylamine, as a yellow powder with mp 90-92 °C.

IR (KBr) cm⁻¹: 3249; 2969; 2946; 2839; 1608; 1594; 1519; 1497; 1456; 1442; 1423; 1327; 1307; 1262; 1237; 1158; 1138; 1094; 1027; 890; 875; 837; 802; 815; 764; 724; 684; 632.

¹H NMR (400 MHz, DMSO-*d*₆) δ (ppm): 2.57 (t, 2H, ³J 7.6 Hz); 2.9 (q, 2H, ³J 6.1 Hz); 3.68 (s, 6H); 3.8 (s, 3H); 6.61 (dd, 1H, ³J 8.1 Hz, ⁴J 1.9 Hz); 6.7 (d, 1H, ⁴J 1.8 Hz); 6.79 (d, 1H, ³J 8.1 Hz); 7.06 (d, 2H, ³J 8.9 Hz); 7.47 (t, 1H, ³J 5.7 Hz); 7.68 (d, 2H, ³J 8.9 Hz);

¹³C NMR (50 MHz, DMSO-*d*₆) δ (ppm): 35.2; 44.7; 55.8; 56; 112.3; 112.9; 114.7; 120.9; 129.1; 131.6; 147.7; 149; 162.5;

CHN: C₁₇H₂₁NO₅S; calculated C 58.10%; H 6.02%; N 3.99% and determined C 58.05%; H 5.99%; N 3.95%.

HPLC: 60/40 acetonitrile/water; λ 254 nm: 97% purity.

2.2.4. N-(3,4-dimethoxyphenethyl)-3,4-dimethoxybenzenesulfonamide (LASSBio-1722, 6d)

The title compound was obtained in 52% yield, by condensing 3,4-dimethoxybenzenesulfonyl chloride with 3,4-dimethoxyphenylethylamine, as a white powder with mp 83-85 °C.

IR (KBr) (cm⁻¹): 3284; 3083; 2967; 2940; 2923; 2838; 1608; 1590; 1511; 1470; 1455; 1421; 1406; 1359; 1318; 1263; 1236; 1188; 1139; 1021; 944; 851; 821; 806; 764; 680; 622.

¹H NMR (200 MHz, DMSO-*d*₆) δ (ppm): 2.59 (t, 2H, ³*J* 7.2 Hz); 2.92 (q, 2H, ³*J* 6.9 Hz); 3.7 (s, 6H); 3.8 (s, 3H); 3.82 (s, 3H); 6.63 (d, 1H, ³*J* 8.2 Hz); 6.72 (s, 1H); 6.8 (d, 1H, ³*J* 8.2 Hz); 7.07 (d, 1H, ³*J* 8.4 Hz); 7.27 (s, 1H); 7.35 (d, 1H, ³*J* 8.4 Hz); 7.49 (t, 1H, ³*J* 5.4 Hz);

¹³C NMR (50 MHz, DMSO-*d*₆) δ (ppm): 35.3; 44.7; 55.9; 56.0; 56.3; 109.9; 111.6; 112.4; 113.1; 120.7; 121; 131.7; 132.6; 147.8; 149.1; 149.2; 152.3.

CHN: C₁₈H₂₃NO₆S; calculated C 56.68%; H 6.08%; N 3.67% and determined C 56.56%; H 6.10%; N 3.70%.

HPLC: 60/40 acetonitrile/water; λ 254nm: 97.1% purity.

2.2.5. N-(3,4-dimethoxyphenethyl)-[1,1'-biphenyl]-4-sulfonamide (LASSBio-1622, 6i)

The title compound was obtained in 70% yield, by condensing 4-biphenyl-4-sulfonyl chloride with 3,4-dimethoxyphenylethylamine, as a yellow powder with mp 84-86 °C.

¹H NMR (400 MHz, DMSO-*d*₆) δ (ppm): 2.63 (t, 2H, ³*J* 7.3 Hz); 3.01 (q, 2H, ³*J* 6.5 Hz); 3.68 (s, 6H); 6.65 (d, 1H, ³*J* 8.1 Hz); 6.74 (s, 1H); 6.81 (d, 1H, ³*J* 8.1 Hz); 7.49 (m, 3H); 7.74 (m, 3H); 7.88 (s, 4H);

¹³C NMR (125 MHz, DMSO-*d*₆) δ (ppm): 35.4; 44.8; 55.9; 56.1; 112.4; 113.1; 121.1; 127.6; 127.7; 127.9; 129; 131.7; 139.1; 139.8; 144.3; 147.9; 149.1;

HPLC: 60/40 acetonitrile/water; λ 254 nm: 98% purity.

HRMS (ESI) (*m/z*) calcd for [C₂₂H₂₃NO₄S + H]⁺ 398,4953 found 398.14164

2.2.6. *N*-(3,4-dimethoxyphenethyl) naphthalene-2-sulfonamide (LASSBio-1611, 6j)

The title compound was obtained in 70% yield, by condensing 2-naphthalenesulfonyl chloride with 3,4-dimethoxyphenylethylamine, as a yellow powder with mp 84-86 °C.

IR (KBr) cm^{-1} : 3284; 3071; 3059; 2997; 2965; 2943; 2921; 2874; 2838; 1605; 1591; 1521; 1472; 1421; 1353; 1318; 1262; 1236; 1157; 1145; 1134; 1073; 1019; 954; 936; 863,816; 757; 677; 637; 621.

^1H NMR (400 MHz, $\text{DMSO-}d_6$) δ (ppm): 2.58 (t, 2H, 3J 7.2 Hz); 2.98 (q, 2H, 3J 7.1 Hz); 3.6 (s, 6H); 6.6 (dd, 1H, 3J 8.1 Hz, 4J 1.8 Hz); 6.68 (s, 1H); 6.75 (d, 1H, 3J 8.1 Hz); 7.66 (m, 2H); 7.77 (m, 2H); 8.01 (d, 1H, 3J 7.9 Hz); 8.09 (d, 1H, 3J 8.9 Hz); 8.11 (d, 1H, 3J 7.7 Hz); 8.4 (s, 1H);

^{13}C NMR (50 MHz, $\text{DMSO-}d_6$) δ (ppm): 35.3; 44.7; 55.8; 55.9; 112.2; 112.9; 120.9; 122.7; 127.7; 128; 128.25; 129.1; 129.6; 129.8; 131.5; 132.2; 134.5; 137.9; 147.7; 149.1;

CHN: $\text{C}_{20}\text{H}_{21}\text{NO}_4\text{S}$; calculated 56.68%; H 6.08%; N 3.67% and determined C 56.48%; H 6.06%; N 3.66%.

HPLC: 60/40 acetonitrile/water; λ 254 nm: 96.3% purity.

2.2.7. *N*-(3,4-dimethoxyphenethyl)-*N*-methyl-4-nitrobenzenesulfonamide (LASSBio-1630, 6e)

The title compound was obtained in 71% yield, by condensing 4-nitrobenzenesulfonyl chloride with *N*-methyl-3,4-dimethoxyphenethylamine, as a white powder with mp 139-141°C.

IR (KBr) cm^{-1} : 3104; 2976; 2963; 2858; 2839; 1608; 1591; 1532; 1518; 1467; 1453; 1422; 1349; 1311; 1166; 1147; 1116; 1023; 941; 927; 856; 819; 782; 765; 737; 705; 684; 617; 602.

^1H NMR (400 MHz, $\text{DMSO-}d_6$) δ (ppm): 2.72 (t, 2H, 3J 7.6 Hz); 2.78 (s, 3H); 3.27 (t, 2H, 3J 7.7 Hz); 3.70 (s, 6H); 6.71 (dd, 1H, 3J 8.1 Hz, 4J 1.9 Hz); 6.77 (d, 1H, 4J 1.9 Hz); 6.82 (d, 2H, 3J 8.1 Hz); 7.98 (d, 2H, 3J 8.8 Hz); 8.36 (d, 2H, 3J 8.8 Hz);

^{13}C NMR (50 MHz, $\text{DMSO-}d_6$) δ (ppm): 33.5; 34.92; 51.60; 55.8; 55.9; 112.2; 113; 121.1; 125; 128.9; 131; 143.5; 147.8; 149.0, 150.1;

CHN: $\text{C}_{17}\text{H}_{23}\text{N}_2\text{O}_6\text{S}$; calculated C 53.67%; H 5.30%; N 7.36% and determined C 53.93%; H 5.32%; N 7.21%.

HPLC: 60/40 acetonitrile/water; λ 254 nm: 97.8 % purity.

2.2.8. *N*- (3,4-dimethoxyphenethyl) -*N*, 2-methylbenzenesulfonamide (LASSBio-1623, 6f)

The title compound was obtained in 68% yield, by condensing *o*-toluenesulfonyl chloride with *N*-methyl-3,4-dimethoxyphenethylamine, as a white powder with mp 54-55 °C.

IR (KBr) cm^{-1} : 3080; 2970; 2949; 2936; 2917; 2834; 1605; 1590; 1515; 1464; 1443; 1417; 1359; 1309; 1263; 1236; 1156; 1141; 1132; 1062; 1025; 950; 933; 856; 814; 788; 789; 755; 676; 630.

^1H NMR (400 MHz, $\text{DMSO-}d_6$) δ (ppm): 2.43 (s, 3H); 2.71 (t, 2H, J 7.8 Hz); 2.78 (s, 3H); 3.3 (q, 2H, J 7.8 Hz); 3.68 (s, 3H); 3.7 (s, 3H); 6.54 (dd, 1H, 3J 8.1 Hz, 4J 1.9 Hz); 6.72 (d, 1H, 4J 1.8 Hz); 6.8 (d, 1H, 3J 8.1 Hz); 7.37 (m, 2H); 7.5 (m, 1H); 7.68 (t, 1H, 3J 5.7 Hz); 7.75 (d, 1H, 3J 7.8 Hz);

¹³C NMR (50 MHz, DMSO-*d*₆) δ (ppm): 20.3; 33.6; 34.2; 51.1; 55.8; 56.0; 112.3; 112.8; 120.9; 126.7; 129.2; 131.2; 133.2; 137.4; 137.4; 147.8; 149.1;

CHN: C₁₈H₂₃NO₄S; calculated C 61.87%; H 6.63%; N 4.01% and determined C 62.04%; H 5.99%; N 4.09%.

HPLC: 60/40 acetonitrile/water; λ 254 nm: 97.7% purity.

2.2.9. N'-(3,4-dimethoxyphenethyl)-4-methoxy-N-methylbenzenesulfonamide (LASSBio-1628, 6g)

The title compound was obtained in 78% yield, by condensing 4-methoxybenzenesulfonyl chloride with N-methyl-3,4-dimethoxyphenethylamine, as a white powder with mp 70-72°C.

IR (KBr) cm⁻¹: 3040; 2943; 2923; 2845; 2830; 1596; 1579; 1518; 1496; 1464; 1449; 1422; 1336; 1298; 1255; 1236; 1152; 1109; 1090; 1028; 1022; 956; 833; 815; 756; 707; 658; 631.

¹H NMR (400 MHz, DMSO-*d*₆) δ (ppm): 2.64 (s, 3H); 2.68 (t, 2H, ³J 7.9 Hz); 3.1 (t, 2H, ³J 8 Hz); 3.7 (s, 6H); 3.82 (s, 3H); 6.7 (dd, 1H, ³J 8.1 Hz, ⁴J 1.3 Hz); 6.78 (s, 1H); 6.83 (d, 1H, ³J 8.1 Hz); 7.09 (d, 2H, ³J 8.7 Hz); 7.66 (d, 2H, ³J 8.7 Hz);

¹³C NMR (50 MHz, DMSO-*d*₆) δ (ppm): 33.5; 35.1; 51.6; 55.8; 55.9; 56.1; 112.3; 113; 114.9; 121; 129.1; 129.7; 131.3; 147.8; 149.1, 162.9;

CHN: C₁₈H₂₃NO₅S; calculated C 59.16%; H 6.34%; N 4.01% and determined C, 59.16%; H 6.34%; N 4.09%.

HPLC: 60/40 acetonitrile/water; λ 254 nm: 98.7 % purity.

2.2.10. N'-(3,4-dimethoxyphenethyl)-3,4-dimethoxy-N-methylbenzenesulfonamide (LASSBio-1610, 6h)

The title compound was obtained in 70% yield, by condensing 3,4-dimethoxybenzenesulfonyl chloride with *N*-methyl-3,4-dimethoxyphenethylamine, as a white powder with mp 78-80°C.

IR (KBr) cm^{-1} : 3114; 3087; 2996; 2959; 2933; 2836; 1588; 1517; 1507; 1465; 1454; 1403; 1424; 1374; 1326; 1261; 1145; 806; 721; 699; 654; 578.

^1H NMR (400 MHz, DMSO- d_6) δ (ppm): 2.7 (m, 5H); 3.15 (t, 2H, 3J 7.4 Hz); 3.72 (s, 6H); 3.82 (s, 6H); 6.71 (d, 1H, 3J 8 Hz); 6.81-6.87 (m, 2H); 7.1-1.19 (m, 2H); 7.33 (d, 1H, 3J 8.4 Hz);

^{13}C NMR (50 MHz, DMSO- d_6) δ (ppm): 33.6; 35.2; 51.6; 55.9; 56.0; 56.3; 56.4; 110.4; 111.9; 112.4; 113.2; 121.1; 121.4; 129.3; 131.5; 147.9; 149.2; 149.3; 152.8;

HPLC: 60/40 acetonitrile/water; λ 254 nm: 96.1% purity.

HRMS (ESI) (m/z) calcd for $[\text{C}_{19}\text{H}_{25}\text{NO}_6\text{S} + \text{H}]^+$ 396,4778 found 396.14703

2.2.11. *N*-(3,4-dimethoxyphenethyl)-*N*-methyl-[1,1'-biphenyl]-4-sulfonamide (LASSBio-1631, 6k)

The title compound was obtained in 55% yield, by condensing biphenyl-4-sulfonyl chloride with *N*-methyl-3,4-dimethoxyphenethylamine, as a white powder with mp 68-70°C.

IR (KBr) cm^{-1} : 3049; 3026; 2992; 2953; 2935; 2873; 2834; 1609; 1591; 1516; 1460; 1449; 1363; 1335; 1301; 1258; 1245; 1158; 1139; 1127; 1091; 1027; 1015; 996; 947; 924; 884; 864; 834; 807; 763; 772; 725; 704; 696; 661; 636.

^1H NMR (400 MHz, DMSO- d_6) δ (ppm): 2.72 (m, 5H); 3.2 (t, 2H, 3J 7.9 Hz); 3.7 (s, 6H); 6.72 (dd, 1H, 3J 8.1 Hz, 4J 1.9 Hz); 6.8 (d, 1H, 4J 1.9 Hz); 6.83 (d, 1H, 3J 8.1 Hz); 7.42 (m, 1H); 7.49 (m, 2H); 7.71 (m, 2H); 7.79 (m, 2H); 7.87 (m, 2H);

¹³C NMR (50 MHz, DMSO-*d*₆) δ (ppm): 33.6; 35.1; 51.66; 55.8; 55.9; 112.3; 113.1; 121.1; 127.5; 127.9; 128.2; 129; 129.6; 131.3; 136.4; 138.9; 144.7; 147.8; 149.1;

HPLC: 60/40 acetonitrile/water; λ 254 nm: 97 % purity.

HRMS (ESI) (*m/z*) calcd for [C₂₃H₂₅NO₄S + H]⁺ 412,5218 found 412.15733

2.2.12. *N*-(3,4-dimethoxyphenethyl)-*N*-methylnaphthalene-2-sulfonamide (LASSBio-1612, 6I)

The title compound was obtained in 73% yield, by condensing 2-naphthalenesulfonyl chloride with *N*-methyl-3,4-dimethoxyphenethylamine, as a white powder with mp 78-80°C.

IR (KBr) cm⁻¹: 3049; 2993; 2933; 2834; 1606; 1590; 1517; 1464; 1455; 1439; 1421; 1337; 1290; 1247; 1234; 1196; 1149; 1129; 1122; 1073; 1028; 946; 927; 854; 821; 747; 716; 653; 637; 618.

¹H NMR (400 MHz, DMSO-*d*₆) δ (ppm): 2.72 (m, 5H); 3.2 (t, 2H, ³*J* 7.9 Hz); 3.7 (s, 6H); 6.71 (dd, 1H, ³*J* 8.1 Hz, ⁴*J* 1.8 Hz); 6.83 (d, 1H, ⁴*J* 1.8 Hz); 6.84 (d, 1H, ³*J* 8.1 Hz); 7.43 (t, 1H, ³*J* 7.3 Hz); 7.5 (t, 2H, ³*J* 7.1 Hz); 7.72 (); 7.8 (m, 2H); 7.87 (d, 1H, ³*J* 8.6 Hz);

¹³C NMR (50 MHz, DMSO-*d*₆) δ (ppm): 33.9; 35.1; 51.6; 55.8; 55.9; 112.3; 113.1; 121.1; 127.5; 128; 128.2; 129; 129.6; 131.3; 136.4; 138.8; 144.7; 147.7; 149.1;

HPLC: 60/40 acetonitrile/water; λ 254 nm: 97.5% purity.

HRMS (ESI) (*m/z*) calcd for [C₂₁H₂₃NO₄S + H]⁺ 386,4846 found 386.14172

2.3. Procedure to prepare of sulfonyl hydrazides (9a-e)

The key intermediates sulfonyl hydrazides **9a** and **9c-b** were obtained in accordance to the methodology previously described in the literature [13,14,15].

2.3.1. 6-methyl-3,4-methylenedioxy-benzenesulfonyl hydrazide (9a)

The title compound was obtained in 84% yield, by reaction with 6-methyl-3,4-methylenedioxy-benzenesulfonyl chloride and hydrazine hydrate, as a white powder with mp 121-123°C [13].

2.3.2. 2-methylbenzenesulfonyl hydrazide intermediate (9b)

The title compound was obtained in 92% yield, by reaction with 2-methylbenzene-1-sulfonyl chloride and hydrazine hydrate, as a colorless oil with mp 144-146°C [14,15].

2.3.3. 4-methoxybenzenesulfonyl hydrazide (9c)

The title compound was obtained in 83% yield, by reaction with 4-methoxybenzene-1-sulfonyl chloride and hydrazine hydrate, as a white powder with mp 150-152°C [14,15].

2.3.4. 4-(trifluoromethyl)benzenesulfonyl hydrazide (9d)

The title compound was obtained in 71% yield, by reaction with 4-(trifluoromethyl) benzenesulfonyl chloride and hydrazine hydrate, as a white powder with mp 149-151°C [14,15].

2.3.5. Benzenesulfonyl hydrazide intermediate (9e)

The title compound was obtained in 98% yield, by reaction with benzenesulfonyl chloride and hydrazine hydrate, as a white powder with mp 138-140°C [14,15].

2.4. General procedure for the synthesis of sulfonyl hydrazones and N-methyl sulfonyl hydrazones

The sulfonyl hydrones **7a-e** were prepared by interconversion of functional groups as previously described by Zapata-Sudo and coworkers [14].

Then, a regioselective alkylation reaction was performed in the presence of K_2CO_3 (1.91 mmol), acetone (5mL) as solvent and methyl iodide (1.91 mmol) as alkyl halide. The reaction was heated at 40 °C and maintained under stirring for 1.5h under reflux. Afterward, the reaction was evaporated under reduced pressure; the residual solid was suspended in 2 mL of ethanol and then poured into cold water. Purification was achieved by simple filtration to obtain the *N*-methyl target compounds **7f-j** [14]. Yields and characterization patterns are described below:

2.4.1. (*E*)-*N'*-(3,4-dimethoxybenzylidene)-6-methylbenzo [d] [1,3] dioxole-5-sulfonyl hydrazone (LASSBio-1624, **7a)**

The title compound was obtained in 72% yield, as a white powder with mp 178-180 °C.

IR (KBr) cm^{-1} : 3201; 3122; 3084; 3044; 2980; 2952; 2912; 2845; 1612; 1601; 1580; 1515; 1498; 1480; 1441; 1424; 1350; 1334; 1321; 1269; 1249; 1233; 1162; 1145; 1043; 1021; 992; 957; 930; 909; 887; 867; 816; 774; 748; 730; 705; 658; 625; 615.

1H NMR (200 MHz, DMSO- d_6) δ (ppm): 2.55 (s, 3H); 3.72 (s, 3H); 3.74 (s, 3H); 6.08 (s, 2H); 6.94 (m, 2H); 7.04 (d, 1H, 3J 8.2 Hz); 7.08 (s, 1H); 7.32 (s, 1H); 7.83 (s, 1H); 11.3 (s, 1H).

^{13}C NMR (50 MHz, DMSO- d_6) δ (ppm): 20.7; 55.9; 56.1; 102.8; 109.1; 109.5; 127.1; 130.6; 133.8; 146.0; 149.5; 151.1; 151.3.

CHN: $C_{17}H_{18}N_2O_6S$; calculated C 53.96%; H 4.79%; N 7.40% and determined C 53.71%; H 4.67%; N 7.50%.

HPLC: 60/40 acetonitrile/water; λ 306 nm: 99.0 % purity.

2.4.2. (E) -N'- (3,4-dimethoxybenzylidene)-2-methylbenzenesulfonyl hydrazone (LASSBio-1847, 7b)

The title compound was obtained in 70% yield, as a yellow powder with mp 141-143 °C.

IR (KBr) cm^{-1} : 3184; 3077; 3065; 3004; 2983; 2937; 2839; 1600; 1580; 1517; 1462; 1440; 1410; 1369; 1360; 1320; 1262; 1240; 1177; 1166; 1131; 1060; 1043; 1021; 1016; 898; 873; 821; 809; 763; 707; 694; 623; 607.

^1H NMR (200 MHz, CDCl_3) δ (ppm): 2.76 (s, 3H); 3.86 (s, 3H); 3.88 (s, 3H); 6.8 (d, 1H, 3J 8.2 Hz); 6.96 (d, 1H, 3J 8.2 Hz); 7.18 (s, 1H); 7.33 (m, 2H); 7.46 (d, 1H, 3J 8.6 Hz); 7.72 (s, 1H); 7.98 (s, 1H); 8.08 (d, 1H, 3J 7.4 Hz).

^{13}C NMR (50 MHz, CDCl_3) δ (ppm): 21.0; 56.0; 56.1; 108.4; 110.7; 122.4; 126.4; 126.5; 130.9; 132.8; 133.5; 136.9; 138.2; 147.7; 149.5; 151.4.

CHN: $\text{C}_{16}\text{H}_{18}\text{N}_2\text{O}_4\text{S}$; calculated C 57.47%; H 5.43%; N 8.83% and determined C 57.41%; H 5.31%; N 8.43%.

HPLC: 60/40 acetonitrile/water; λ 306 nm: 98.5 % purity.

2.4.3. (E) -N'- (3,4-dimethoxybenzylidene) -4-methoxybenzenesulfonyl hydrazone (LASSBio-1845, 7c).

The title compound was obtained in 70% yield, as a yellow powder with mp 141-143 °C.

IR (KBr) cm^{-1} : 3198; 3098; 3082; 3085; 3013; 2977; 2943; 2839; 1598; 1578; 1521; 1499; 1453; 1429; 1407; 1353; 1317; 1271; 1263; 1242; 1162; 1132; 1095; 1021; 970; 941; 901; 837; 803; 781; 765; 703; 629; 615.

¹H NMR (200 MHz, CDCl₃) δ (ppm): 3.82 (s, 3H); 3.86 (s, 6H); 6.79 (d, 1H, ³J 8.2 Hz); 6.96 (m, 3H); 7.2 (s, 1H); 7.75 (s, 1H); 7.92 (d, 2H, ³J 8.9 Hz), 8.31 (s, 1H).

¹³C NMR (50 MHz, CDCl₃) δ (ppm): 55.7; 56.0; 56.1; 108.7; 110.8; 114; 122.3; 126.5; 130; 130.2; 148.7;

CHN: C₁₆H₁₈N₂O₅S; calculated C 54.85%; H 5.18%; N 7.99% and determined C 54.74%; H 5.11%; N 8.00%.

HPLC: 60/40 acetonitrile/water; λ 306 nm: 99.4 % purity.

2.4.4. N'-(3,4-dimethoxybenzylidene)-4-(trifluoromethyl) benzenesulfonyl hydrazide (LASSBio-1849, 7d).

The title compound was obtained in 66% yield, as a white powder with mp 87-89°C.

¹H NMR (200 MHz, CDCl₃) δ (ppm): 3.87 (s, 6H); 6.81 (d, 1H, ³J 8.1 Hz); 7.02 (d, 1H, ³J 8 Hz); 7.2 (s, 1H); 7.77 (m, 3H); 8.13 (d, 2H, ³J 8.1 Hz); 8.39 (s, 1H).

¹³C NMR (50 MHz, CDCl₃) δ (ppm): 56.1; 56.2; 108.6; 110.9; 120.6; 122.6; 126; 126.3 (q, ²J_{CF} 3.6 Hz); 128.6; 135.1 (q, ¹J_{CF} 33 Hz); 138.8; 142.1; 149.5; 151.7.

HPLC: 60/40 acetonitrile/water; λ 306 nm: 99.6 % purity.

HRMS (ESI) (m/z) calcd for [C₁₆H₁₅F₃N₂O₄S + H]⁺ 389,3694 found 389.07748

2.4.5. (E) -N'-(3,4-dimethoxybenzylidene) benzenesulfonyl hydrazone (LASSBio-1851, 7e).

The title compound was obtained in 66% yield, as a white powder with mp 87-89 °C.

¹H NMR (200 MHz, CDCl₃) δ (ppm): 3.77 (s, 6H); 6.71 (d, 1H); 6.92 (d, 1H, ³J 8.2 Hz); 7.1 (s, 1H); 7.44 (m, 3H); 7.68 (s, 1H); 7.92 (d, 2H, ³J 8.1 Hz); 8.39 (s, 1H).

¹³C NMR (50 MHz, CDCl₃) δ (ppm): 56.0; 108.5; 110.8; 122.4; 126.4; 128; 129.1; 133.4; 138.5; 148.8; 149.4; 151.4.

CHN: C₁₅H₁₆N₂O₄S; calculated C 56.24%; H 5.03%; N 8.74% and determined C 56.27%; H 5.04%; N 8.96%.

HPLC: 60/40 acetonitrile/water; λ 306 nm: 99.5 % purity

2.4.6. (E) -N²- (3,4-dimethoxybenzylidene)-N, 6-methylbenzo [d] [1,3] dioxole-5-sulfonyl hydrazone (LASSBio-1632, 7j)

The title compound was obtained in 64% yield, as a white powder with mp 156-158 °C.

¹H NMR (200 MHz, CDCl₃) δ (ppm): 2.55 (s, 3H); 3.23 (s, 3H); 3.81 (s,s, 6H); 5.93 (s, 2H); 6.62 (s, 1H); 6.74-6.76 (d, 1H); 6.93-6.95 (d, 1H); 7.17 (s, 1H); 7.40 (s, 1H); 7.45 (s, 1H).

¹³C NMR (50 MHz, CDCl₃) δ (ppm): 21.1; 32.5; 55.7-55.9; 102.1; 106.1 – 151.3.

CHN: C₁₈H₂₀N₂O₆S; calculated C 55.09%; H 5.14%; N 7.14% and determined C 55.17%; H 5.14%; N 7.22%.

HPLC: 60/40 acetonitrile/water; λ 306 nm: 98% purity.

2.4.7. N²-(3,4-dimethoxybenzylidene)-N,2-methylbenzenesulfonyl hydrazone (LASSBio-1848, 7f).

The title compound was obtained in 70% yield, as a white powder with mp 84-86 °C.

¹H NMR (200 MHz, CDCl₃) δ (ppm): 2.64 (s, 3H); 3.24 (s, 3H); 3.77 (s, 3H); 3.8 (s, 3H); 6.73 (d, 1H, *J* 7 Hz); 6.92 (d, 1H, *J* 7 Hz); 7.1 (s, 1H, *J* 7 Hz); 7.21 (m, 2H); 7.35 (d, 1H, *J* 7 Hz); 7.44 (s, 1H); 7.92 (d, 1H, *J* 8 Hz).

¹³C NMR (50 MHz, CDCl₃) δ (ppm): 21.1; 32.4; 55.8; 56.1; 108.2; 110.8; 122; 126.1; 127.5; 130.8; 132.8; 133.2; 135.9; 138.8; 142.1; 149.4; 150.9.

CHN: C₁₇H₂₀N₂O₄S; calculated C 58.60%; H 5.79%; N 8.04% and determined C 58.31%; H 5.86%; N 8.18%.

HPLC: 60/40 acetonitrile/water; λ 306 nm: 99.6 % purity

2.4.8. *N*-(3,4-dimethoxybenzylidene)-4-methoxy-*N*-methylbenzene-sulfonyl hydrazone (LASSBio-1846, 7g).

The title compound was obtained in 70% yield, as a white powder with mp 141-143 °C.

¹H NMR (200 MHz, CDCl₃) δ (ppm): 3.18 (s, 3H); 3.84 (s, 3H); 3.9 (s, 3H); 3.93 (s, 3H); 6.85 (d, 1H, *J* 7 Hz); 6.96 (d, 2H, *J* 7 Hz); 7.07 (d, 1H, *J* 7 Hz); 7.29 (s, 1H); 7.61 (s, 1H); 7.83 (d, 2H, *J* 7.8 Hz).

¹³C NMR (50 MHz, CDCl₃) δ (ppm): 34.1; 55.7; 56.0; 108.7; 110.8; 114.1; 122.1; 127.4; 128; 130.5; 145.5; 149.9; 151.1; 163.4.

CHN: C₁₇H₂₀N₃O₄S; calculated C 56.03%; H 5.53%; N 7.69% and determined C 55.73%; H 5.52%; N 7.69%.

HPLC: 60/40 acetonitrile/water; λ 306 nm: 99.6 % purity

2.4.9. *N*-(3,4-dimethoxybenzylidene)-4-(trifluoromethyl)-*N*-methyl-4-(trifluoromethyl)benzenesulfonyl hydrazone (LASSBio-1850, 7h).

The title compound was obtained in 66% yield, as a white powder with mp 87-89 °C.

¹H NMR (200 MHz, CDCl₃) δ (ppm): 3.15 (s, 1H); 3.83 (s, 3H); 3.84 (s, 3H); 6.78 (d, 1H, ³J 8.2 Hz); 7.01 (d, 1H, ³J 8.2 Hz); 7.17 (s, 1H); 7.57 (s, 1H); 7.69 (d, 2H, ³J 8.1 Hz); 7.95 (d, 2H, ³J 8.1 Hz).

¹³C NMR (50 MHz, CDCl₃) δ (ppm): 34.1; 56.1; 56.1; 108.7; 111; 120.6; 122.3; 126 (q, ²J_{CF} 3.6 Hz); 126.9; 129; 134.8 (q, ¹J_{CF} 33 Hz); 140.1; 146.7; 149.5; 151.5.

CHN: C₁₇H₁₇F₃N₂O₄S; calculated C 50.74%; H 4.26%; N 6.96% and determined C 50.53%; H 4.31%; N 7.04%.

HPLC: 60/40 acetonitrile/water; λ 306 nm: 98.5 % purity.

2.4.10. N-(3,4-dimethoxybenzylidene)-N-methylbenzenesulfonyl hydrazone (LASSBio-1852, 7i).

The title compound was obtained in 60% yield, as a white powder with mp 108-110 °C.

¹H NMR (200 MHz, CDCl₃) δ (ppm): 3.13 (s, 3H); 3.83 (s, 3H); 3.85 (s, 3H); 6.77 (d, 1H, ³J 8.2 Hz); 7.01 (d, 1H, ³J 8.2 Hz); 7.2 (s, 1H); 7.44 (m, 3H); 7.54 (s, 1H); 7.82 (d, 2H, ³J 8.1 Hz).

¹³C NMR (50 MHz, CDCl₃) δ (ppm): 34.1; 56.1; 56.1; 108.7; 110.9; 122.2; 127.3; 128.4; 128.9; 133.3; 136.6; 145.7; 149.5; 151.2.

HPLC: 60/40 acetonitrile/water; λ 306 nm: 99% purity.

HRMS (ESI) (m/z) calcd for [C₁₆H₁₈N₂O₄S + H]⁺ 335,3981 found 335.10567

2.5. X-ray diffraction experiments

The crystals were obtained by the slow evaporation method from **7j** and **7a** under a saturating condition at 298K. After X days, a suitable yellow single crystal was observed for both samples.

Intensity data were collected at room temperature (293K) with graphite monochromated MoKa radiation ($\lambda=0.71073 \text{ \AA}$), using an Enraf-Nonius Kappa-CCD diffractometer. The unit cell was refined using the software Collect [36] and Scalepack [37], and the final cell parameters were obtained on all reflections. Data were collected up to 24.41° in θ for Lassbio-1624 and 27.88° for **7j** in θ , giving 12,489 and 16,238 Bragg reflections respectively. Data reduction was carried out using the software Denzo-SMN and Scalepack, and the program XdisplayF was used for visual representation of the data. No significant absorption coefficient (0.227 mm^{-1} for **7a** and 0.211 mm^{-1} for **7a**) was observed. Thus, a semi-empirical absorption correction based on equivalents was applied [38]. The structure was solved using the software SHELXS-97 [39], and refined using the software SHELXL-97, where the C, N and O atoms were clearly solved, and full-matrix least square refinement of these atoms with anisotropic thermal parameters was carried out. The hydrogen atoms were positioned stereochemically and were refined with the riding model. The details concerning the data collection and structure refinement were prepared using WinGX (version 1.80.05) [40]. The ORTEP-3 [41] program was used to prepare the figures.

The complete crystallographic data were deposited at the Cambridge Crystallographic Data Centre as supplementary publication no. CCDC 1944285 and no. CCDC 1944286 for LASSBio-1624 and LASSBio-1632 respectively. Copies of the data are available on application to The Director, CCDC, 12 Union Road, Cambridge CB2 1EZ, UK (e-mail: deposit@ccdc.cam.ac.uk or <http://www.ccdc.cam.ac.uk>).

2.6. Solubility Assay

The solubility assay was performed considering the absorptivity of compounds under ultraviolet spectroscopy as described by Schneider and coworkers. The assay wavelength was determined by the λ_{max} characteristic of each compound. Saturated aqueous solutions were prepared (0.8-1.0 mg/mL) and were kept under stirring for 4 hours at 37 °C. The supernatant was filtered in 0.45 mm filters and transferred to a quartz cuvette (10 mm) to spectra acquisition. Solubility was determined by linear regression using as excel graph plots, solutions prepared by dilutions of the original solution in methanol. The data were obtained in triplicates and the mean values were used to the graph plots. The correlation coefficient (R^2) values were between 0.9982 and 1.

2.7. Chemical Stability Assay

The chemical stability studies were conducted at two different pH (2.0 and 7.4). The stock solutions of compounds were prepared at 5 mM to 10 mM concentrations and solubilized in DMSO. Standard solutions were prepared adding 2 μL of the stock solution in 249 μL acid buffer (KCl 0.2 M and HCl 0.2 M; pH = 2.0) or neutral buffer (PBS, pH = 7.4) in eppendorf microtube. The mixture was placed in a water bath at 37 °C under vigorous stirring for 0, 30, 60 and 120 minutes. At the end of each time reaction, 249 μL of basic buffer (phosphate buffer, pH = 8.4) was added to neutralize the pH of the medium in experiments using acidic buffer. Extraction of the compound was performed by adding 1.0 mL of acetonitrile. The organic phase was separated, filtered and analyzed by HPLC-PDA (acetonitrile / water mobile phase and 50% to 60%).

2.8. Pharmacological Evaluation

2.8.1 Animals

Male A/J mice (18-20 g) were obtained from the Oswaldo Cruz Foundation breeding colony and used in accordance with the guidelines of the Committee on Use of Laboratory Animals of the Oswaldo Cruz Institute (CEUA-IOC/FIOCRUZ, license L-027/2016). Mice were housed in groups of four in a temperature-, humidity-, and light-controlled (12 h light: 12 h darkness cycle) colony room. Mice were given *ad libitum* access to food and water.

Adult guinea-pigs (*Cavia porcellus*) from the Professor Thomas George Bioterium at Federal University of Paraíba (UFPB), weighing 300 – 500 g, were used. Animals were maintained on a 12-h light-dark cycle, under controlled ventilation and temperature with free access to food and water. Actions on reducing pain, stress, and any suffering were taken in accordance to the local ethical guidelines for animal usage. All experimental procedures had been approved and performed in accordance to the Animal Research Ethic Committee of UFPB guidelines (CEPA/UFPB license 0610/11).

2.8.2. Drugs

Methacholine, LPS (*Escherichia coli*, serotype 0127:B8) and nembutal were purchased from Sigma Chemical Co. Pancuronium bromide, isoflurane and sodium thiopental were purchased from Cristalia (São Paulo, Brazil). LPS, pancuronium bromide, nembutal and sodium thiopental were diluted in 0.9% NaCl sterile solution. Methacholine was diluted in PBS. All work solutions were freshly prepared by dissolving the compounds in DMSO 0.1% and further diluting them in 0.9% NaCl. All solutions were freshly prepared immediately before use.

Arachidonic acid (AA), carbamylcholine hydrochloride (CCh), ovalbumin (OVA) (grade V), rolipram (**1**), aluminum hydroxide (Al(OH)₃) and Cremophor

EL™ were purchased from Sigma-Aldrich (Brazil). CCh was dissolved in distilled water and AA was dissolved in ethanol (95%). Compounds were solubilized in Cremophor EL™ (3%) and distilled water at the concentration of 10^{-2} M, being again diluted in distilled water as required for each experimental protocol. The final content of Cremophor EL™ in the organ solution never exceeded 0.01% (v/v). The carbogen mixture (95% O₂ and 5% CO₂) was acquired from White Martins (Brazil).

2.8.3. PDE4 activity evaluation in vitro

PDE4A, 4B, 4C and 4D activities were measured by employing an IMAP TR-FRET protocol (kit from Molecular Devices, Sunnyvale, CA, USA). Briefly, the enzymatic reactions were carried at room temperature in a 96-well black plate by co-incubating 25 μ L of 200 nM FAM-cAMP (R7513), 5 μ L of putative inhibitory compounds and 20 μ L of the PDE4 isoform dissolved in assay buffer (R7364) for 1 h. All enzymes were obtained from human recombinant sources (MDS PHARMA), whereas the other reagents were purchased from Molecular Devices. Fluorescence polarization intensity was measured at 485 nm excitation and 520 nm emission using a microplate reader, SpectraMax M5 (Molecular Devices, Sunnyvale, CA, USA). Cilomilast was dissolved in dimethyl sulfoxide (DMSO) at a final concentration of 0.1%. At this condition, the vehicle had no significant effect on PDE4 activity. The concentration of drugs that produced 50% inhibition of substrate hydrolysis (IC₅₀) was calculated by nonlinear regression analysis from concentration response curves, using the GraphPad Prism Software, version 5.0 (USA).

2.8.4. LPS-induced lung inflammation

Mice were anesthetized with isoflurane aerosol and then stimulated with LPS (25 μ g/25 μ L) or 0.9% NaCl sterile solution by intranasal instillation. Treatment with test compounds (6.25 and 25 μ mol/kg) or cilomilast (3 μ mol/kg) was performed by gavage, 1 h before LPS provocation. Untreated mice received vehicle (0.1% DMSO) by gavage. The analyses were carried out 24 h after LPS stimulation.

2.8.5. Evaluation of airway hyper-reactivity

Following general anesthesia with nembutal[®] (60 mg/kg, i.p.), and neuromuscular blockade (pancuronium bromide, 1 mg/kg, i.v.), lung elastance of mice was measured using an invasive whole-body plethysmography (Buxco Electronics, United States) as previous described [12]. Briefly, after the mechanical ventilator was connected to the mouse through an endotracheal tube, it was stabilized for 5 min and increasing concentrations of methacholine (3, 9, and 27 mg/ml) were aerosolized for 5 min each. Baseline lung elastance was assessed with aerosolized phosphate-buffered saline (PBS).

2.8.6. Lung TNF- α quantification

Tumour necrosis factor (TNF)- α was quantified in the right lung samples using a commercial ELISA kit according to the manufacturer's instructions (R&D Systems).

2.8.7. Relaxant effect in non-sensitized and sensitized guinea pig's trachea

The animals were randomly divided into two groups: non-sensitized and sensitized. On the 1st day, guinea pigs were treated with OVA (60 μ g/mL, i.p. and s.c.), as a sensitizing agent, and with Al(OH)₃ (1 mg/mL, i.p. and s.c.), as an adjuvant. Both were dissolved on saline solution (NaCl 0,9 %). After, on the

8th day, the animals were individually placed in a closed polyacrylic box coupled to an ultrasonic nebulizer and nebulized with an OVA solution (OVA 3 mg/mL + saline) for 5 minutes. Then, on the 15th day, guinea pigs were nebulized again with another OVA solution (OVA 1 mg/mL + saline) for 1 minute. Lastly, from the days 21st to 25th the animals were euthanized by cervical dislocation followed by sectioning of cervical vessels for experimentation. Non-sensitized animals were subjected to the same treatment procedure but received only saline (adapted from Espinoza *et al.*, 2013) [42].

After evaluation of epithelium integrity using arachidonic acid [34], the tracheal rings from non-sensitized and sensitized animals were contracted with CCh (1.0 mM) and when a stable contraction was obtained. Rolipram, LASSBio-448 (**1**) and LASSBio-1632 (**3j**) were individually and cumulatively added to the preparation. Relaxation was expressed as pEC₅₀ and E_{max}, calculated from the obtained concentration-response curves.

2.9. Statistical analysis

All data are presented as means \pm standard error of the mean (SEM) and statistical analysis involving two groups was done, with Student's t test, whereas ANOVA followed by the Newman-Keuls-Student's t test or by Bonferroni's test were used to compare more than 2 groups. *P* values of 0.05 or less were considered significant (the null hypothesis was rejected when $p < 0.05$).

2.10. Parallel artificial membrane permeability assay (PAMPA)

To determine the permeability profile (passive diffusion) of the target, Parallel artificial membrane permeability assay (PAMPA) was selected as passive permeation prediction method. Commercial drugs (obtained from

Sigma Aldrich) were used to validate both PAMPA-TGI and PAMPA-BBB, as well as high purity solvents. Donor 96-well plate MultiScreen with 0,45 μM pore size (catalog No. MAIPS4510), acceptor 96-well plate MultiScreen (catalog No. MAMCS9610), and 0,22 μM pores size filter (catalog No SLGS033) were obtained from Millipore®. Results were determined by UV reading in 3-5 different wavelengths peaks for each compound previously determined (UV-reader SpectraMax M3 from Molecular Devices®).

In order to predict the permeability into the gastrointestinal tract, *L*- α -phosphatidylcholine was used (CAS Number 8002-43-5 from Sigma-Aldrich®) in *n*-dodecane (20 mg/mL) solution. All compounds, including commercial, were stocked in 10mM DMSO solutions before diluted in pH 6,6 PBS to a 0,05 mM (DMSO 5%, v/v) in donor plate. Acceptor plate 96-well were filled with pH 7,4 PBS under constant agitation during 8-hour incubation period at room temperature [43], as well as the donor and acceptor plate wells receive 180 μL of buffered solution. Compounds were classified according to the percentage of absorbed fraction ($F_a\%$), such as: high intestinal permeability (70-100%), medium permeability (30-69%) or low permeability (0-29%), previously described by KANSY & colabs (1998) [43].

PAMPA was also used to predict blood-brain barrier passive permeability. Commercial drugs and test compounds were dissolved in ethanol 99,8% (1mg/mL). Stock solutions were then diluted in pH 7,4 PBS/EtOH (70:30 v/v). Each 96-well of donor plate were covered with 5 μL of *n*-dodecane-PBL solution (20mg/mL) porcine polar membrane lipid extract (PBL) (catalog No. 141101P, Avanti Polar Lipids) purchased from Sigma-Aldrich®.

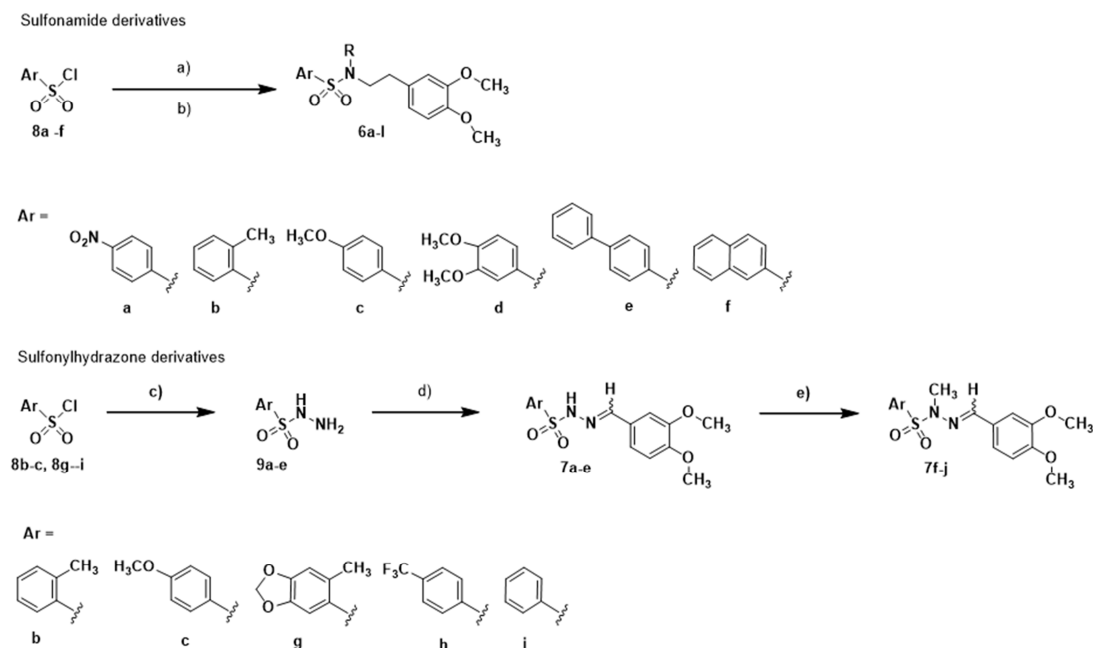
Donor plate was filled with 180 μ L of each compound solution; 180 μ L of PBS/EtOH (70/30) were added to the acceptor plate to form the donor-acceptor "sandwich". Incubation time was 2h45min at room temperature. Thereafter, 96-well plates were separated and each well were read by UV reader in 3-5 different wavelengths for each compound previously determined. Results were presented as positive (CNS+) when $Pe > 4.0$, uncertain permeation (CNS+/-) when $Pe < 4.0$ to > 2.0 or non-permeable (CNS-) when $Pe < 2.0$. Standard cutoff values were established following the pattern equations criteria from Crivori *et al.* (2000) and Di *et al.* (2003) [44,45].

3. Results and Discussion

3.1. Synthesis

Compounds were synthesized as depicted in Scheme 1. The congeneric sulfonamide series was prepared in one step by condensation reaction between the sulfonyl chloride derivatives (**8a-f**) and the 3,4-dimethoxyphenethylamine or *N*-methyl-3,4-dimethoxyphenethylamine, following the methodology previously described [10,11].

The sulfonyl hydrazones were synthesized in two linear steps, exploring the sulfonyl hydrazides **9a-e** as a key intermediate. These intermediates were obtained from the hydrazinolysis of the sulfonyl chloride derivatives (**8b-c**, **8g-i**) [13,14]. Condensation with functionalized aldehyde was performed to give the target compounds **7a-e**, in good yields, following previously methodology described by Zapata-Sudo and co-workers [14]. The *N*-methyl-sulfonyl hydrazones (**7f-j**) were synthesized by *N*-methylation of compounds **7a-e** by classical *N*-alkylation reaction, using methyl iodide and sodium carbonate in acetone (Scheme 1) [16].



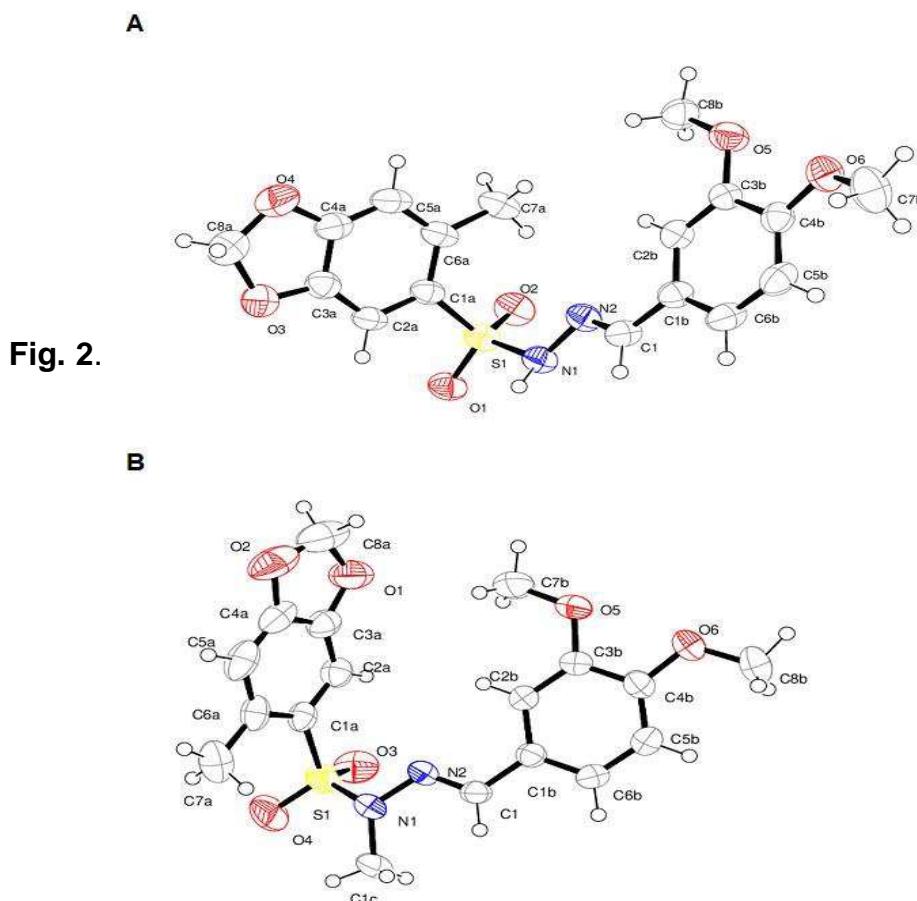
Scheme 1. Reagents and conditions: a) 3,4-dimethoxyphenethylamine, CH_2Cl_2 , Et_3N , r.t., 2-5h, 52-73%; b) *N*-methyl-3,4-dimethoxyphenethylamine, CH_2Cl_2 , Et_3N , r.t., 2-5h, 55-78%; c) $\text{NH}_2\text{NH}_2 \cdot \text{H}_2\text{O}$, CHCl_3 , 0°C , 2h, 71-95 %; d) functionalized aldehydes, EtOH , r.t., HCl cat., 2h, 60-92 %; e) K_2CO_3 , ICH_3 , acetone, 40°C , 1.5 h, 60-98%.

All compounds had their chemical structure elucidated by nuclear magnetic resonance (NMR) of hydrogen (^1H) and carbon (^{13}C), mass spectrometry (MS) and infrared spectroscopy (IR). Bearing in mind that sulfonyl hydrazone can be obtained as a mixture of diastereoisomer (*E* and *Z*), X-ray diffraction experiments were performed to unambiguously characterize the relative configuration of the imine double bond ($\text{N}=\text{CH}$). Due to the difficulty of obtaining all compounds in the crystalline form, compounds **7a** and **7j**, respectively, were chosen as representatives of the sulfonyl hydrazone series to perform X-ray diffraction studies. As anticipated by the chemical displacement of the single imine hydrogen observed in the ^1H -NMR spectra of the all synthesized sulfonyl hydrazones, the crystallographic structures of **7a** and **7j** confirmed the *E* stereochemistry proposed to the imine double bond (Fig. 2).

Considering that all sulfonyl hydrazones were obtained through the same synthetic methodology and their chemical shift similarity regarding the imine function (N=CH) in ^1H and ^{13}C NMR spectra analysis, the results obtained from X-ray analysis to **7a** and **7j** were extrapolated for all synthesized sulfonyl hydrazones. This assumption was also based on previous data from literature [17-19].

Besides the elucidation of the imine stereochemistry, X-ray diffraction analysis contributed to show the comparative differences between the conformation of the sulfonyl hydrazone scaffold **7a** and its *N*-methyl analogue **7j**. While a planar conformation was observed for **7a**, which clearly reflect the antiperiplanar relationship between the hydrogen and the oxygen atom of sulfonyl hydrazone framework ($\text{RSO}_2\text{NHN}=\text{CHR}$), a folded conformation was detected for **7j**.

This classical methyl effect, well characterized in acylhydrazone molecules [10], had not previously been demonstrated for sulfonyl hydrazones. The introduction of a methyl subunit linked to the nitrogen of the sulfonyl hydrazone framework resulted in the rotation of the $\text{SO}_2\text{N}(\text{CH}_3)\text{R}$ fragment by 180° , assuming a synperiplanar relationship between the methyl group and the oxygen atom of sulfonyl hydrazone framework, as shown by Newman's projections (Fig. 3). The folded conformation of **7j** can be probably due to the steric effect generated by the additional methyl group [20].



Crystallographic structures of the sulfonyl hydrazone compounds **7a** (A) and **7j** (B) by *Ortep 3* representation.

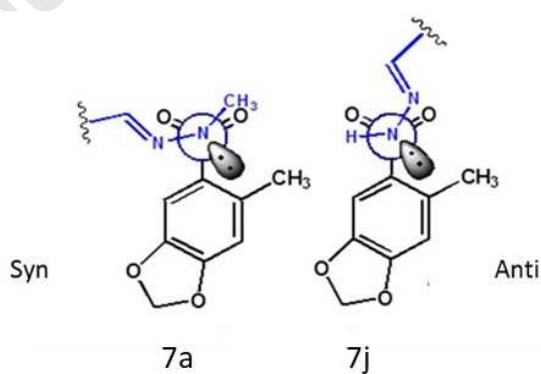


Fig. 3. Newman's projections illustrating the conformational modifications observed on the crystallographic structures of the sulfonyl hydrazone **7a** and its methyl homologous **7j**.

In order to obtain information about the drug likeness profile of the sulfonamides and sulfonyl hydrazones designed by modifications in the

previous prototype LASSBio-448 (**5**), their cLogP, tPSA and pKa were calculated *in silico* and their aqueous solubility were determined by ultraviolet spectrometry [14, 21]. The data obtained are summarized in supplementary material (Table S1 and S2).

The cLogP (<5) and tPSA (< 140 Å²) calculated for compounds **5**, **6a-l** and **7a-j** (Tables S1 and S2) are in agreement with Lipinski's [22] (no violation to the "rule of five") and Veber's [23] rules, allowing the assumption that all sulfonamides and sulfonyl hydrazones could be predicted having good oral bioavailability potential.

Regarding compounds solubility, the molecular modifications introduced at benzodioxole fragment of LASSBio-448 (**5**) have resulted in analogues with better aqueous solubility, as exemplified by compounds **6a-6d**. The attempt to replace benzodioxole ring by naphthyl or biphenyl has reduced markedly the solubility (**6i-6j**). As expected, all methyl homologous were less soluble than their parent compounds. None of the modifications have changed, significantly, the pKa of sulfonamide's analogues (Table S1). The conformational restriction and planarity introduced by the replacement of ethylene subunit by an imine group have reduced the aqueous solubility of sulfonyl hydrazones **7a-7e**. As observed in sulfonamide series, methyl-homologation reduced compounds' solubility (**7f-7j**) (Table S2). The pKa values calculated *in silico* for sulfonyl hydrazones revealed their greater acidity compared to the sulfonamides.

The chemical stability of sulfonamides and sulfonyl hydrazones was investigated in buffer solution in pH values that simulate gastric acid (pH = 2) and serum content (pH 7.4) [14]. Like the prototype **5**, all sulfonamides showed

great chemical stability at pH= 2.0 and pH = 7.4 (Fig. 4). On the other hand, the sulfonyl hydrazones were stable only in pH=7.4. Their instability in acid condition was demonstrated to be dependent of the imine hydrolysis, generating the hydrazide and the aldehyde chemical precursors [24]. The analysis of chromatograms obtained by HPLC-DAD confirmed this hypothesis, revealing the signal characteristic of aldehyde formation (Fig. 5).

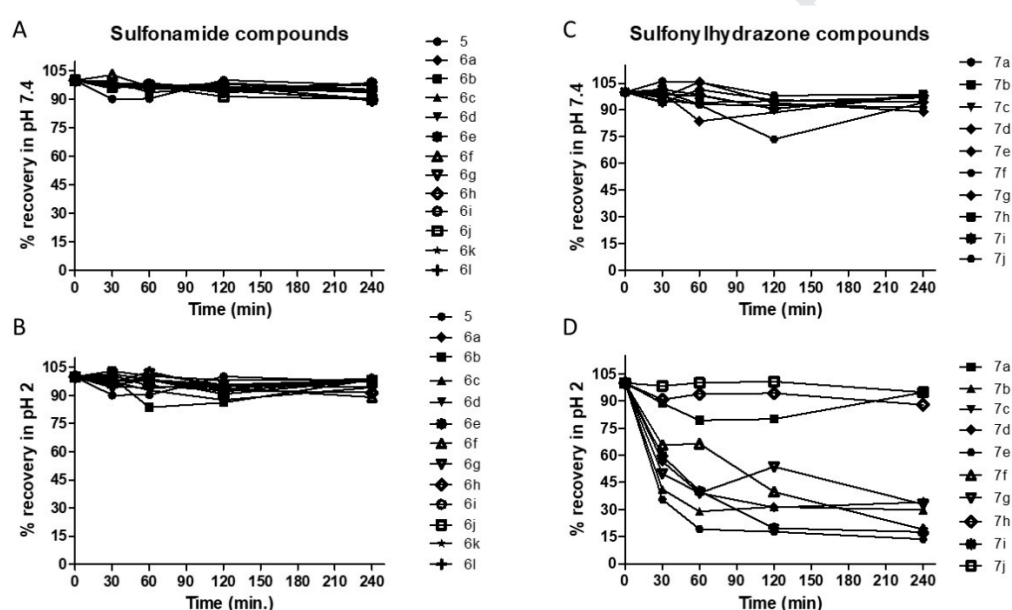


Fig. 4. Chemical stability A) Sulfonamides at pH 7.4; B) Sulfonamides at pH 2; C) Sulfonyl hydrazones at pH 7.4; D) Sulfonyl hydrazones at pH 2. Experiments performed in duplicate / quadruplicate. Reading performed CLAE-PDA [Shimadzu- LC20A; Kromasil C-18 column (4.6mm x 250mm); detector SPD-M20A (Diode Array); flow rate: 1 ml / min]; Mobile phase: Acetonitrile: water, 60%. Wavelength: 254 nm and 308 nm. Calculations were performed according to the peak area values of the analytes.

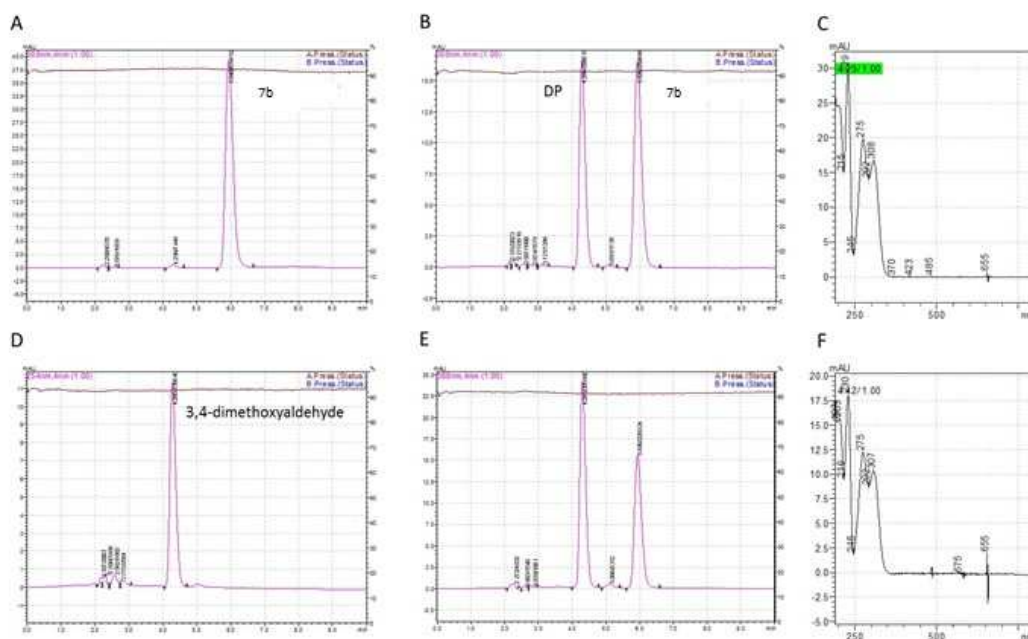


Fig. 5: Chromatograms of chemical stability of compound **7b**, representative of sulfonyl hydrazone series. A) chemical stability of **7b** at pH 2, time 0min, retention time (rt) 5.9 min. ; B) chemical stability of **7b** after 60min of incubation in buffer at pH 2; degradation product (DP) rt 4.2 min.; C) UV spectrum of degradation product (DP); D) chromatogram of 3,4-dimethoxyaldehyde at 100uM, rt 4.2 min; E) co-elution of 3,4-dimethoxyaldehyde with the chemical stability sample of **7b**; F) UV spectrum of aldehyde represented in D. Experiments carried out in duplicate. Reading performed CLAE-PDA [Shimadzu- LC20A; Kromasil C-18 column (4.6mm x 250mm); detector SPD-M20A (Diode Array); flow rate: 1 ml / min]; Mobile phase: Acetonitrile: water, 60%. Wavelength: 308 nm.

3.2. Biology

3.2.1. *In vitro* studies

The efficacy of sulfonamides and sulfonyl hydrazones, designed in order to optimize the prototype LASSBio-448 (**5**), was addressed first by evaluating the capacity of these compounds to inhibit the four human PDE4 isoforms *in vitro*, i.e. PDE4A, PDE4B, PDE4C, and PDE4D, using an IMAP-FP assay. PDE4A, 4B and 4D, but not 4C, have been shown to play a pivotal role in human inflammatory diseases [25,26], while the blockade of PDE4D has been strongly associated with emesis, the most important side effect of this class of

drug [26]. They were tested at a screening concentration of 10 μ M. Compounds able to inhibit the PDE4 activity in $\geq 50\%$ were further evaluated for potency determination.

As demonstrated in Table 1, in general, the homologation by the introduction of a methyl group on the nitrogen of sulfonamide and sulfonyl hydrazone frameworks resulted in an improvement of PDE4 inhibition activity. The presence of electron withdrawing group (e.g. NO_2 and CF_3), as a substituent of the position 4 in the phenyl ring linked to sulfonamide or sulfonyl hydrazone sulfur atom, resulted in loss of activity. While the presence of the electron donating group (e.g. OCH_3) contributed favorably to the activity. The replacement of ethylene unit by an imine fragment in the structure of LASSBio-448 (**5**) was detrimental for the PDE4 inhibition (**5** *viz-a-viz* **7a**, Tables 1 and 2).

However, the methyl homologous of the sulfonyl hydrazone **7a** (i.e. **7j**) was the most active compound during the screening assays. This data, when associated to the noticeable differences between the conformational aspects of compounds **7a** and **7j** (Figs. 2 and 3), can indicate **7j** as a frozen analogue of LASSBio-448 (**5**) that can mimic its bioactive conformation while compound **7a** cannot.

Table 1. PDE4 recombinant isoform inhibition by cilomilast, the prototype LASSBio-448 (**5**) and its sulfonamide and sulfonyl hydrazone analogues.

Compounds	PDE4A1A	PDE4B1	PDE4C	PDE4D3
Cilomilast (2)	91.3 ± 0	91.3 ± 2.7	98.5 ± 3.6	98.8 ± 2.1
LASSBio-448 (5)	11,8 ± 1,13	Inactive	21,3 ± 1,3	Inactive
(6a)	Inactive	13.8 ± 13.8	Inactive	Inactive
(6b)	6.1 ± 9.0	Inactive	Inactive	Inactive
(6c)	11.0 ± 1.6	Inactive	20.7 ± 4.2	23.8 ± 0.3
(6d)	11,3 ± 6,6	Inactive	26,0 ± 4,2	13,6 ± 4,4
(6e)	Inactive	Inactive	19.0 ± 19.0	Inactive
(6f)	25.9 ± 0.3	26.5 ± 1.1	Inactive	27.6 ± 0.9
(6g)	43.0 ± 5.6	33.0 ± 0.4	23.5 ± 3.1	35.6 ± 0.5
(6h)	36.1 ± 1.7	12.0 ± 4.3	16.4 ± 4.6	31.1 ± 1.1
(6i)	14.8 ± 0.9	Inactive	Inactive	10.8 ± 0.6
(6j)	30.4 ± 1.2	Inactive	12.1 ± 5.2	9.1 ± 2.1
(6k)	46.8 ± 0.5	7.1 ± 1.0	26.6 ± 26.6	56.3 ± 2.5
(6l)	89.9 ± 10.1	12.2 ± 1.7	30.1 ± 1.0	50.1 ± 2.1
(7a)	Inactive	Inactive	Inactive	8.8 ± 0.6
(7b)	8,0 ± 10,9	Inactive	19,5 ± 2,4	15,9 ± 5,3
(7c)	35,2 ± 3,5	Inactive	40,2 ± 1,2	20,2 ± 2,8
(7d)	Inactive	Inactive	29,0 ± 5,5	19,7 ± 0,0
(7e)	11,9 ± 6,7	Inactive	14,6 ± 2,7	Inactive
(7f)	16,2 ± 2,4	Inactive	39,3 ± 5,2	26,1 ± 1,5
(7g)	31,5 ± 5,2	Inactive	43,0 ± 1,0	12,8 ± 3,7
(7h)	37,5 ± 8,3	Inactive	35,4 ± 7,4	22,2 ± 8,8
(7i)	Inactive	Inactive	15,7 ± 1,4	12,4 ± 5,6
(7j)	90.4 ± 0.2	22.7 ± 2.4	25.5 ± 10.2	90.7 ± 1.5

All compounds were used at the concentration of 10 µM. Percentual values of inhibition of PDE4 isoforms were represented as mean ± SEM from 3 distinct experiments. Values below 5% of inhibition were indicated as inactive.

Considering the data depicted in Table 1, the sulfonamides **6k** and **6l** and the sulfonyl hydrazone **7j** were selected to establish their concentration-response curves on PDE4 isoforms.

The evaluation pointed out a selective on-target activity for **6l** and **7j** by their blockade of PDE4A and PDE4D, with no significant effect on both PDE4B and PDE4C isoforms. The compound **6k** also shown to be active, but only against the PDE4D, and at the limit of the established cut off (Table 1). As expected, cilomilast (**2**) inhibited PDE4A, 4B, 4C and 4D showing IC₅₀ values of 0.20 ± 0.02 μM, 0.40 ± 0.07 μM, 0.30 ± 0.01 μM, and 0.30 ± 0.01 μM (mean ± SEM) (n=3), respectively. Comparative of potency and maximal effect data with cilomilast (**2**) is given in Table 4. The compound **7j** displayed slightly lower 2.5- and 2.3-fold potency than cilomilast concerning PDE4A and PDE4D, respectively. However, its maximal effect (E_{MAX}) was quite comparable to the one of cilomilast as targeting PDE4A, and slightly lower (E_{MAX} = 93% vs 99%) as targeting PDE4D. The compound **6l** was shown to be 15-fold less potent than cilomilast (**2**) in inhibiting PDE4A, but about 118-fold less potent than the reference compound in respect to the blockade of PDE4D. Its efficacy upon PDE4A was quite comparable with that of cilomilast (**2**), but for **6l** E_{MAX} was clearly lower (63% vs 99%) as targeting PDE4D. The second sulfonamide analogue **6k** was 69-fold less potent than the reference compound in inhibiting PDE4D. The E_{MAX} values for compound **6k** concerning PDE4A and PDE4D were 65 and 60%, respectively (Table 2). Since side effects of PDE4 inhibitors can, at least in part, be related with on-target PDE4D activity [27,28], the low efficacy of the sulfonamide analogues towards this isoenzyme should be an advantageous for an anti-PDE4 agent.

Table 2. Potency (IC_{50}) and maximal effect (E_{MAX}) values obtained from concentration-response curves of 6k, 6l, 7j and cilomilast (2) in PDE4A and PDE4D activity *in vitro*.

Compound	PDE4A		PDE4D	
	IC_{50} (μ M)	E_{MAX} (%)	IC_{50} (μ M)	E_{MAX} (%)
Cilomilast (2)	0.2 ± 0.02	99 ± 0	0.3 ± 0.01	99 ± 0.4
(6l)	$3.0 \pm 0.06^*$	97 ± 2	$35.3 \pm 0.03^*$	$63 \pm 0.4^*$
(6k)	n.d.	$65 \pm 1^*$	$20.8 \pm 0.02^*$	$60 \pm 0.1^*$
(7j)	0.5 ± 0.01	100 ± 0	0.7 ± 0.02	$93 \pm 0.5^*$

Values were represented as mean \pm SEM from 3 distinct experiments.

* $p < 0.05$ compared to cilomilast treatment.

3.2.2. *In vivo* studies

Investigations into the *in vivo* effectiveness of candidate to selective PDE4A and D inhibitors using a short-term murine model of LPS-induced lung inflammation were performed. Comparative data with the not sub-type selective cilomilast is given in Table 5. Like the reference compound, **6l**, **6k** and **7j**, administered orally 1 h before provocation, strongly inhibited airway hyper-reactivity by LPS, as attested by aerolized methacholine 24 h post-challenge. This is a surprising finding for candidate compounds acting on PDE4A and 4D only, since PDE4B is shown to be a pivotal PDE4 isoform in mediating inflammation by LPS [29]. LPS-induced production of pro-inflammatory cytokines, like TNF- α and others, is associated to harmful responses, including airway hyper-reactivity [10,19,30]. In our conditions, intranasal instillation of LPS significantly increased TNF- α lung tissue levels from 41.5 ± 8.6 pmol/mg ($n=7$)

(controls) to 535.7 ± 59.5 pmol/mg ($n=7$) ($p<0.05$). As shown in Table 3, cilomilast (**2**) ($3 \mu\text{mol/kg}$) abolished the LPS-induced TNF- α response, whereas the sulfonyl hydrazone **7j** dose-dependently decreased TNF- α production in 49% and 86% after doses of 6.25 and 25 $\mu\text{mol/kg}$. In contrast, the sulfonamides **6l** and **6k**, even at a dose 8-fold higher than cilomilast, were clearly less efficacious compared to the reference compound, leading to a reduction in TNF- α response of no more than 59% and 55%, respectively.

Concerning these analogues, blockade of TNF- α production was shown to be irrelevant for their protective effect upon LPS-induced airway hyper-reactivity as seen at the lower dose tested (6.25 $\mu\text{mol/kg}$) (Table 3). Taken together, these results suggest that the development of more selective PDE4A isozyme inhibitors, such as **7j**, a sulfonyl hydrazone analogue of the previous prototype LASSBio-448 (**5**), can be of potential importance in controlling disease states dominated by endotoxin-induced lung inflammation. Also, despite the loss of efficacy on pro-inflammatory cytokine production, the development of more selective PDE4A isoenzyme inhibitors, such as the sulfonamides **6l** and **6k**, may be a useful strategy concerning those clinical conditions where bronchoconstriction and airway hyper-reactivity is present.

Table 3. Effect of compounds **6l**, **6k**, **7j** and cilomilast (**2**) on LPS-induced airway hyper-reactivity (AHR) and TNF- α production in the lung tissue.

Compound	Dose ($\mu\text{mol/kg}$)	% Inhibition	
		AHR	TNF- α
Cilomilast (2)	3	94 \pm 3*	98.9 \pm 0.7*
(6l)	6.25	95 \pm 4*	0.0 \pm 0.0
	25	97 \pm 2*	58.9 \pm 12.7*
(6k)	6.25	95 \pm 2*	22.2 \pm 6.8
	25	80 \pm 6*	55.1 \pm 17.5*
(7j)	6.25	99 \pm 0*	48.7 \pm 7.2*
	25	97 \pm 6*	85.9 \pm 5.6*

Values were represented as mean \pm SEM from 6 mice. * p <0.05 as compared to an untreated group.

Further, considering the two main pathophysiological components of asthma disorder, it means inflammation and airways hyperresponsiveness, we investigated the relaxant effect of **7j** in a non-sensitized and sensitized guinea pigs' model. The model was selected considering that guinea pigs is known to present a notable homology with humans in terms of airways and lungs anatomy, pathophysiology and in response to contractile and bronchodilators agents [31,22].

The comparative potency and efficacy of LASSBio-448 (**5**) and its sulfonyl hydrazone analogue **7j** to relax the tracheal preparations of non-sensitized and sensitized guinea pigs is shown in Table 4. In order to assess the airway epithelium involvement, the experiments were conducted in its presence (E+) and absence (E-) in both non-sensitized and sensitized guinea pigs. The airway epithelium is a relevant regulator of airway tonus, being

responsible for the production of important bronchodilators, such as nitric oxide and prostacyclin [33-35].

On non-sensitized animals, LASSBio-448 (**5**) and **7j** relaxed the guinea pig trachea pre-contracted with CCh (1.0 mM) in both the presence ($pEC_{50} = 4.53 \pm 0.12$, 5.08 ± 0.26 , respectively) and absence of epithelium ($pEC_{50} = 4.36 \pm 0.08$, 5.09 ± 0.21 , respectively). Similarly, on sensitized guinea pigs, LASSBio-448 and **7j** relaxed the guinea pig trachea pre-contracted with CCh (1.0 mM) in both the presence ($pEC_{50} = 4.61 \pm 0.2$, 5.19 ± 0.21 , respectively) and absence of epithelium ($pEC_{50} = 4.60 \pm 0.11$, 5.50 ± 0.15 , respectively). The results clearly demonstrated that LASSBio-448 (**5**) and its sulfonyl hydrazone analogue **7j** presented their relaxant effects independently of the epithelium presence on guinea pig trachea (Fig. 6). Therefore, it is plausible that their action occurs directly on airways smooth muscle. However, **7j** and its prototype **5** were less potent than the non-selective PDE4 inhibitor rolipram (Fig. 6).

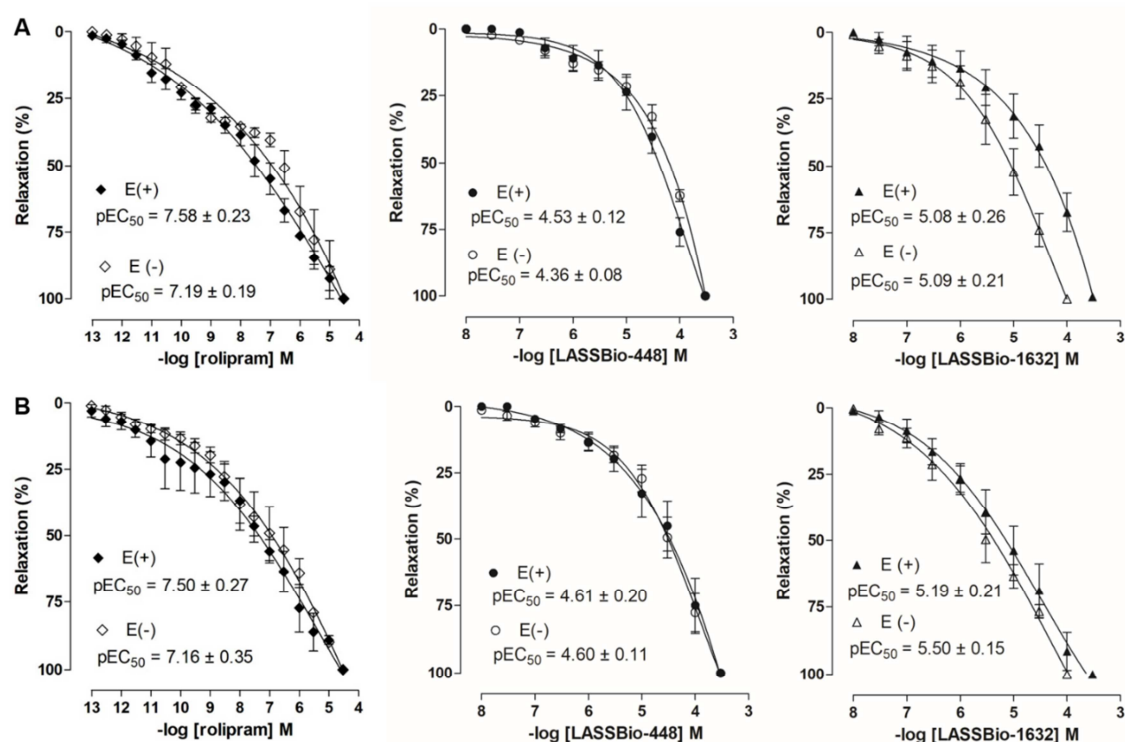


Fig. 6. Effect of rolipram (**1**), LASSBio-448 (**5**) and **7j** on the tonic contractions induced by CCh (1.0 mM) in the presence (E+) or absence (E-) of functional epithelium on non-sensitized (A) and sensitized guinea pigs (B). Symbols and vertical bars represent the mean and S.E.M., respectively.

3.3. Parallel artificial membrane permeability assay (PAMPA)

The comparative permeability profile of **7j** and its parent analogue (**5**, LASSBio-448) was determined using Parallel artificial membrane permeability assay (PAMPA) [44-49]. As demonstrated in Table 4, the prototype **5** and **7j** showed high permeability through gastrointestinal tract with 93.74% and 99.30% of experimental absorption range.

Considering the ability of compound **7j** to inhibit PDE4D and the association of this isoenzyme with the emetic effects of PDE4 inhibitors, we also

investigated the capability of **7j** to cross the blood-brain barrier (BBB) by using PAMPA-BBB assay [45,49]. As depicted in Table 5, **7j** displayed high experimental BBB permeability (Pe) across BBB through passive diffusion. This result was similar to roflumilast, being both compounds classified as CNS+, and it was different from the prototype **5** (LASSBio-448) that showed a smaller Pe ($3,46 \times 10^{-6}$ cm/s) value.

Table 4. Permeability coefficient of standard drugs, used as a control, and of target compounds by the PAMPA-TGI assay.

Compound	Literature permeability (10^{-6} cm/s)	Experimental permeability (10^{-6} cm/s)	Experimental absorption range (%)	Classification
Aciclovir	0.06	0.08	2,98	Low
Aspirin	3.8	1.69	47.36	Medium
Atenolol	0.1	0.11	4.22	Low
ketoconazol	3.3	4.93	84.68	High
Cumarin	22.9	22.65	99.98	High
Diclofenac	12.5	13.01	99.28	High
Hidrocortisone	3.4	2.16	55.93	Medium
Prednisone	5.7	3.09	69.16	Medium
Ranitidine	0.5	0.38	13.48	Low
Sulfasalazine	0.3	0.45	15.5	Low
Verapamil	7.4	6.45	91.40	High
(2)	-	7.29	93.74	High
(7j)	-	13.08	99.30	High
Roflumilast (3)	-	5.28	86.58	High

Table 5. Permeability coefficient of standard drugs, used as a control, and of target compounds by the PAMPA-BBB assay.

Compound	Literature Permeability (10^{-6} cm/s)	Experimental Permeability (10^{-6} cm/s)	Classification
Atenolol	0.8	0.6	CNS -
Caffeine	1.3	1.28	CNS -
Diazepam	16	15,30	CNS +
Enoxacin	0.9	0.56	CNS -
Hydrocortisone	1.9	1.72	CNS -
Ofloxacin	0.8	0.54	CNS -
Testosterone	17	10.55	CNS +
Verapamil	16	8.18	CNS +
LASSBio-448 (1)	-	3.46	CNS +/-
LASSBio-1632 (8a)	-	6.52	CNS +
Roflumilast	-	8.05	CNS +

Conclusion

In summary, we describe here the attempt to optimize the anti-PDE4 activity of the prototype LASSBio-448 (**5**), through the design of two series of analogues: the sulfonamides (**6a-l**) and sulfonyl hydrazones (**7a-7j**). **7j** (LASSBio-1632) was identified as new PDE4 inhibitor, with a selective effect upon PDE4A and PDE4D isoenzymes. This sulfonyl hydrazone was shown to modulate the hyper-reactivity (AHR) and TNF- α production in the lung tissue, being effective at an 8-fold higher dose than the reference compound. It also relaxed guinea pig trachea on non-sensitized and sensitized animals, arising as a new anti-asthmatic lead-candidate with great TGI permeability. In view of

compound **7j** PDE4 inhibition profile and its *in silico* prediction as BBB permeate drug, the ability of **7j** to induce emesis and its efficacy in others models for human inflammatory diseases are now under investigation.

Acknowledgments

The authors would like to thank CNPq (BR), FAPERJ (BR), CAPES (BR) and INCT-INOVAR (BR, 573.564/2008-6 and E-26/170.020/2008) for fellowship and financial support.

References

- [1] N. Kumar, A. M. Goldminz, N. Kim, A. B. Gottlieb, Phosphodiesterase 4-targeted treatments for autoimmune diseases, *BMC Med.* 11 (2013) 96, <https://doi.org/10.1186/1741-7015-11-96>.
- [2] A. Chiricozzi, D. Caposiena, V. Garofalo, M. V. Cannizzaro, S. Chimenti, R. Saraceno, A new therapeutic for the treatment of moderate-to-severe plaque psoriasis: apremilast, *Expert Rev. Clin. Immunol.* 12 (3) (2016) 237-249, <https://doi.org/10.1586/1744666X.2016.1134319>.
- [3] H. Li, J. Zuo, W. Tang, Phosphodiesterase-4 Inhibitors for the Treatment of Inflammatory Diseases, *Front. Pharmacol.* 9 (2018) 1048, <https://doi.org/10.3389/fphar.2018.01048>.
- [4] J. Luo, I. Yang, J. Yang, D. Yang, B. Liu, B. Liang, C. Liu, Efficacy and safety of phosphodiesterase 4 inhibitors in patients with asthma: A systematic review and meta-analysis, *Respirology* 23 (5) (2018) 467-477, <https://doi.org/10.1111/resp.13276>.
- [5] E. V. Schalkwyk, K. Strydom, Z. Williams, L. Venter, S. Leichtl, C. S. Wirlitsch, D. Bredenbröker, P. G. Bardin, Roflumilast, an oral, once-daily phosphodiesterase 4 inhibitor, attenuates allergen-induced asthmatic reactions, *J. Allergy Clin. Immunol.* 116 (2) (2005) 292-298, <https://doi.org/10.1016/j.jaci.2005.04.023>.
- [6] T. Goto, A. Shiina, T. Murata, M. Tomii, T. Yamazaki, K. Yoshida, T. Yoshino, O. Suzuki, Y. Sogawa, K. Mizukami, N. Takagi, T. Yoshitomi, M. Etori, H. Tsuchida, T. Mikkaichi, N. Nakao, M. Takahashi, H. Takahashi, S. Sasaki, Identification of the 5,5-dioxo-7,8-dihydro-6*H*-thiopyrano[3,2-*d*]pyrimidine derivatives as highly selective PDE4B inhibitors, *Bioorg. Med. Chem. Lett.* 24 (3) (2014) 893-989, <https://doi.org/10.1016/j.bmcl.2013.12.076>.
- [7] M. Kobayashi, M. Kobayashi, S. Kubo, K. Shiraki, M. Iwata, Y. Hirano, Y. Ohtsu, K. Takahashi, Y. Shimizu, Therapeutic Potential of ASP3258, a Selective Phosphodiesterase 4 Inhibitor, on Chronic Eosinophilic Airway Inflammation, *Pharmacology* 90 (2012) 223-232. doi: 10.1159/000342380.

- [8] M. A. Giembycz, Cilomilast: a second generation phosphodiesterase 4 inhibitor for asthma and chronic obstructive pulmonary disease, *Expert Opin. Investig. Drugs*, 10 (7) (2001) 1361-1379, doi: 10.1517/13543784.10.7.1361.
- [9] A. S. Kalgutkar, E. Choo, T. J. Taylor, Disposition of CP-671, 305, a selective phosphodiesterase 4 inhibitor in preclinical species. *Xenobiotica* 34 (8) (2004) 755-770.
- [10] I. K. C. Nunes, E. T. Souza, S. V. S. Cardozo, V. F. Carvalho, N. C. Romeiro, P. M. R. Silva, M. A. Martins, E. J. Barreiro, L. M. Lima, Synthesis, Pharmacological Profile and Docking Studies of New Sulfonamides Designed as Phosphodiesterase-4 Inhibitors, *PLoS One* 11 (10) (2016) e0162895, <https://doi.org/10.1371/journal.pone.0162895>.
- [11] L. M. Lima, E. J. Barreiro, Bioisosterism: a useful strategy for molecular modification and drug design, *Curr Med Chem.* 12 (1) (2005) 23-49, <https://doi.org/10.2174/0929867053363540>.
- [12] E. J. Barreiro, A. E. Kümmerle, C. A. M. Fraga, The methylation effect in medicinal chemistry, *Chem. Rev.* 111 (9) (2011) 5215-5246, <https://doi.org/10.1021/cr200060g>.
- [13] L. M. Lima, E. G. Amarante, A. L. P. Miranda, C. A. M. Fraga, E. J. Barreiro, Synthesis and Antinociceptive Profile of Novel Acidic Sulphonylhydrazone Derivatives From Natural Safrole, *Pharm. Pharmacol. Comm.*, 5 (1999) 673-678.
- [14] G. Zapata-Sudo, I. K. C. Nunes, J. S. C. Araujo, M. M. Trachez, T. F. Silva, F. P. Costa, R. T. Sudo, E. J. Barreiro, L. M. Lima, Synthesis, solubility, plasma stability, and pharmacological evaluation of novel sulfonylhydrazones designed as anti-diabetic agents, *Drug Des. Devel. Ther.* 10 (2016) 2869-2879, <https://doi.org/10.2147/DDDT.S108327>.
- [15] Y. Xinzhang, L. Xingwei, W. Boshun, Palladium-catalyzed desulfitative arylation of azoles with arylsulfonyl hydrazides, *Org. Biomol. Chem.*, 10 (2012) 7479-7482.
- [16] A. Barco, S. Benetti, G. P. Pollini, A Facile Alkylation of Ethyl 2-Oxocyclopentanecarboxylate, *Synthesis-Stuttgart* 5 (1973) 316, <https://doi.org/10.1055/s-1973-22208>.
- [17] L. M. Lima, M. M. Trachez, J. S. C. Araujo, J. S. Silva, D. N. Amaral, R. T. Sudo, E. J. Barreiro, G. Zapata-Sudo, Novel Partial Agonist of PPAR-Gamma for Treatment of Diabetic Neuropathy in Rats, *J. Diabetes Metab.* 5 (7) (2014) 392, <https://doi.org/10.4172/2155-6156.1000392>.
- [18] G. Palla, G. Predieri, P. Domiano, C. Vignali, W. Turner, Conformational behaviour and E/Z isomerization of N-acyl and N-arylohydrazones, *Tetrahedron* 42 (13) (1986) 3649-3654. [https://doi.org/10.1016/S0040-4020\(01\)87332-4](https://doi.org/10.1016/S0040-4020(01)87332-4).
- [19] A. E. Kümmerle, M. Schmitt, S. V. Cardozo, C. Lugnier, P. Villa, A. B. Lopes, N. C. Romeiro, H. Justiniano, M. A. Martins, C. A. M. Fraga, J. J. Bourguignon, E. J. Barreiro, Design, synthesis, and pharmacological evaluation of N-acylhydrazones and novel conformationally constrained compounds as

- selective and potent orally active phosphodiesterase-4 inhibitors, *J. Med. Chem.* 55 (17) (2012) 7525-7545, <https://doi.org/10.1021/jm300514y>.
- [20] A. E. Kümmerle, J. M. Raimundo, C. M. Leal, G. S. Silva, T. L. Balliano, M. A. Pereira, C. A. Simone, R. T. Sudo, G. Zapata-Sudo, C. A. M. Fraga, E. J. Barreiro, Studies towards the identification of putative bioactive conformation of potent vasodilator arylidene N-acylhydrazone derivatives, *Eur. J. Med. Chem* 44 (13) (2009) 3649-3654, <https://doi.org/10.1016/j.ejmech.2009.04.044>.
- [21] P. Schneider, S. S. Hosseiny, M. Szczotka, V. Jordan, K. Schlitter, Rapid solubility determination of the triterpenes oleanolic acid and ursolic acid by UV-spectroscopy in different solvents, *Phytochem. Letters* 2 (2) (2009) 85-87, <https://doi.org/10.1016/j.phytol.2008.12.004>.
- [22] C. A. Lipinski, F. Lombardo, B. W. Dominy, P. J. Freaney, P.J., Experimental and computational approaches to estimate solubility and permeability in drug discovery and development settings, *Adv. Drug Deliver. Rev.* 23 (1-3) (1997) 23-25, [https://doi.org/10.1016/S0169-409X\(96\)00423-1](https://doi.org/10.1016/S0169-409X(96)00423-1)
- [23] D. F. Veber, S. R. Jonson, H. Y. Cheng, B. R. Smith, K. W. Ward, K. D. Kopple, Molecular Properties That Influence the Oral Bioavailability of Drug Candidates, *J. Med. Chem.* 45 (12) (2002) 2615-2626, <https://doi.org/10.1021/jm020017n>.
- [24] F. A. Carey, R. J. Sundberg *Advanced Organic Chemistry: Part A: Structure and Mechanisms*, Springer, University of Virginia, fifth ed., 2008.
- [25] C. P. Page, Phosphodiesterase Inhibitors for the Treatment of Asthma and Chronic Obstructive Pulmonary Disease, *Int. Arch. Allergy Immunol.* 165 (3) (2014) 152-164, <https://doi.org/10.1159/000368800>.
- [26] C. Lugnier, Cyclic nucleotide phosphodiesterase (PDE) superfamily: a new target for the development of specific therapeutic agents, *Pharmacol. Ther.* 109 (3) (2006) 366-398, <https://doi.org/10.1016/j.pharmthera.2005.07.003>.
- [27] A. Robichaud, P. B. Stamatiou, N. Lachance, P. Jolicoeur, R. Rasori, C. C. Chan, Assessing the emetic potential of PDE4 inhibitors in rats, *Br. J. Pharmacol.* 135 (2002) 113-118, <https://doi.org/10.1038/sj.bjp.0704457>.
- [28] A. Robichaud, P. B. Stamatiou, S. L. Jin, N. Lachance, D. MacDonald, F. Laliberte, S. Liu, Z. Huang, M. Conti, C. C. Chan, Deletion of phosphodiesterase 4D in mice shortens α_2 -adrenoceptor-mediated anesthesia, a behavioral correlate of emesis, *J. Clin. Invest.* 110 (7) (2002) 1045-1052, <https://doi.org/10.1172/JCI15506>.
- [29] S. L. Jin, M. Conti, Induction of the cyclic nucleotide phosphodiesterase PDE4B is essential for LPS-activated TNF-alpha responses. *Proc. Natl. Acad. Sci. USA* 99 (11) (2002) 7628-7633, <https://doi.org/10.1073/pnas.122041599>.
- [30] M. L. C. Barbosa, T. J. F. Ramos, A. C. S. Arantes, M. A. Martins, P. M. R. Silva, E. J. Barreiro, L. M. Lima, Synthesis and Pharmacological Evaluation of Novel Phenyl Sulfonamide Derivatives Designed as Modulators of Pulmonary Inflammatory Response, *Molecules* 17 (12) (2012) 14561-14672, <https://doi.org/10.3390/molecules171214651>.
- [31] A. R. Ressmeyer, A. K. Larsson, E. Vollmer, S. E. Dahlen, S. Uhlig, C. Martin, Characterisation of guinea pig precision-cut lung slices: comparison with

- human tissues, *Eur. Respir. J.* 28 (2006) 603-611, <https://doi.org/10.1183/09031936.06.00004206>.
- [32] D. Wright, P. Sharma, M. H. Ryu, P. A. Rissé, M. Ngo, H. Maarsingh, C. Koziol White, A. Jha, A. J. Halayko, A. R. West, Models to study airway smooth muscle contraction *in vivo*, *ex vivo* and *in vitro*: implications in understanding asthma, *Pulm. Pharmacol. Ther.* 26 (2013) 24-36, <https://doi.org/10.1016/j.pupt.2012.08.006>.
- [33] D. B. Insuela, J. B. Daleprane, L. P. Coelho, A. R. Silva, P. M. Silva, M. A. Martins, V. F. Carvalho, Glucagon induces airway smooth muscle relaxation by nitric oxide and prostaglandin E₂, *J. Endocrinol.* 225 (3) (2015) 205-217, <https://doi.org/10.1530/JOE-14-0648>.
- [34] D. A. Knight, S. T. Holgate, The airway epithelium: structural and functional properties in health and disease, *Respirology* 8(4) (2003) 432-446, <https://doi.org/10.1046/j.1440-1843.2003.00493.x>.
- [35] E. Tschirhart, N. Frossard, C. Bertrand, Y. Landry, Arachidonic acid metabolites and airway epithelium-dependent relaxant factor, *J. Pharmacol. Exp. Ther.* 243 (1987) 310-316, PMID: 3118008.
- [36] V. F. Sardela, C. S. Anselmo, I. K. C. Nunes, G. R. A. Carneiro, G. R. C. Santos, A. R. Carvalho, B. J. Labanca, D. S. Oliveira, W. D. Ribeiro, A. L. D. Araújo, M. C. Padilha, C. K. F. Lima, V. P. Sousa, F. R. Aquino-Neto, H. M. G. Pereira, Zebrafish (*Danio rerio*) water tank model for the investigation of drug metabolism: Progress, outlook, and challenges. *Drug. Test. Anal.* 10 (11-12) (2018) 1657-1669, <https://doi.org/10.1002/dta.2523>.
- [37] Enraf-Nonius Collect. Nonius BV, Delft, Netherlands, 1997.
- [38] Z. Otwinowski, W. Minor, Processing of X-ray diffraction data collected in oscillation mode, *Methods Enzymol.* 276 (1997) 307-326, [https://doi.org/10.1016/S0076-6879\(97\)76066-X](https://doi.org/10.1016/S0076-6879(97)76066-X).
- [39] R. H. Blessing, An empirical correction for absorption anisotropy, *Acta Cryst.* 51 (1995) 33-38, <https://doi.org/10.1107/S0108767394005726>.
- [40] G. M. Sheldrick, SHELXS-97, University of Göttingen, Göttingen, Germany, 1997.
- [41] L. J. Farrugia, WinGX suite for small-molecule single-crystal crystallography, *J. Appl. Crystallogr.* 32 (4) (1999) 837-838, <https://doi.org/10.1107/S0021889899006020>.
- [42] L. J. Farrugia, ORTEP-3 for Windows - a version of ORTEP-III with a Graphical User Interface (GUI), *J. Appl. Crystallogr.* 30 (1997) 565, <https://doi.org/10.1107/S0021889897003117>.
- [43] J. Espinoza, L. M. Montañó, M. Perusquía, Nongenomic bronchodilating action elicited by dehydroepiandrosterone (DHEA) in a guinea pig asthma model, *J. Steroid Biochem. Mol. Biol.* 138 (2013) 174-182, <https://doi.org/10.1016/j.jsbmb.2013.05.009>.
- [44] Kansy, M., Senner, F., Gubernator, K. Physicochemical High Throughput Screening: Parallel Artificial Membrane Permeation Assay in the Description of

Passive Absorption Processes. *J. Med. Chem.*, 41 (1998), 1007-1010. [https://doi.org/10.1016/s0223-5234\(03\)00012-6](https://doi.org/10.1016/s0223-5234(03)00012-6)

[45] Crivori, P. Cruciani, G., Carrupt, P. A., Testa, B. Predicting Blood-Brain Barrier Permeation from Three-Dimensional Molecular Structure. *J. Med. Chem.*, 43 (2000) 2204-2216. <https://doi.org/10.1021/jm990968+>.

[46] Di, L., Kerns, E. H., Fan, K., Mcconnell, O. J., Carter, G. T. High throughput artificial membrane permeability assay for blood–brain barrier. *European Journal of Medicinal Chemistry*, v. 38, n. 3, p. 223-232, 2003. [https://doi.org/10.1016/s0223-5234\(03\)00012-6](https://doi.org/10.1016/s0223-5234(03)00012-6).

[47] Sun, H., Nguyen, K., Kerns, E., Yan, Z., Yu, K. R., Shah, P., Jadhav, A., Xu, X. Highly predictive and interpretable models for PAMPA permeability. *Bioorg. Med. Chem.* 25 (2017), 1266–1276. <https://doi.org/10.1016/j.bmc.2016.12.049>

[48] Cabrera-pérez, M. A., Sanz, M. B., Sanjuan, V. M., González-álvarez, M., Álvarez I. G. Importance and applications of cell- and tissue-based in vitro models for drug permeability screening in early stages of drug development. *Cell and Tissue Based in vitro Culture Models* (2016), 3-29. <https://doi.org/10.1016/B978-0-08-100094-6.00002-X>.

[49] Blokland, A., Heckman, P., Vanmierlo, T., Schreiber, R., Paes, D., Prickaerts, J. Phosphodiesterase Type 4 Inhibition in CNS Diseases. *Trends Pharmacol Sci*, 40 (2019), 971-985. <https://doi.org/10.1016/j.tips.2019.10.006>

Highlights

- A new selective PDE4A and PDE4D inhibitor
- Good drug-like properties
- blockade of airway hyper-reactivity (AHR) and TNF- α production in the lung tissue
- relaxant effects on guinea pig trachea

Journal Pre-proof

Declaration of interests

The authors declare that they have no known competing financial interests or personal relationships that could have appeared to influence the work reported in this paper.

The authors declare the following financial interests/personal relationships which may be considered as potential competing interests:

For the record I sign this declaration on behalf of all authors of the manuscript entitled: "Discovery of a new selective PDE-4A and PDE4D inhibitor by lead-optimization approach on the prototype LASSBio-448"

A handwritten signature in black ink, appearing to read 'Adrian K. ...', is written over a large, faint, diagonal watermark that says 'Journal Pre-proof'.